4-8-2016

Renewable Energy Investment Planning and Policy Design

Alireza Ghalebani
University of South Florida, alireza@mail.usf.edu

Renewable Energy Investment Planning and Policy Design

by

Alireza Ghalebani

A dissertation submitted in partial fulfillment
of the requirements for the degree of
Doctor of Philosophy in Industrial Engineering
Department of Industrial and Management Systems Engineering
College of Engineering
University of South Florida

Major Professor: Tapas K. Das, Ph.D.
Yogi D Goswami, Ph.D.
Michael Fountain, Ph.D.
Andrei Barbos, Ph.D.
Bo Zeng, Ph.D.
Hui Yang, Ph.D.

Date of Approval:
March 29, 2016

Keywords: Integer Programming, Analytics, Power Systems, Net Zero Energy Building, Financial Incentives

DEDICATION

To my parents, legends of love, determination, and integrity.

ACKNOWLEDGMENT

My sincere gratitude is hereby extended to my knowledgeable supervisor, Dr. Tapas K Das for all his support for different dimensions of my research during the past four years. I appreciate how he challenged me throughout my academic program and his never accepting less than my best efforts.

I am very thankful to my supervisory committee, Dr. Yogi D Goswami, Dr. Michael Fountain, Dr. Andrei Barbos, Dr. Bo Zeng, and Dr. Hui Yang, for graciously sharing their knowledge and experience and supporting my academic endeavour. My special appreciation goes to Dr. Goswami for offering his unparalleled experience in solar energy which significantly widened my understanding in this domain. I am also very appreciative to Dr. Fountain for intellectually supporting my entrepreneurial journey.

I would like to thank Dr. Andrei Barbos, who not only gave me a lot of insights in economics and in particular game theoretical analysis, but also has been a great friend. Special thanks to Dr. Bo Zeng for enhancing my optimization skills and Dr. Hui Yang who helped me explore data analytic even more.

I offer my sincere regards to Dr. Peter Fabri, Dr. Dmitry Khavinson, and all whom I have learnt from in any context.

Finally to Anna, my appreciation is beyond words.

TABLE OF CONTENTS

LIST OF TABLES

LIST OF FIGURES

ABSTRACT

In this dissertation, we leverage predictive and prescriptive analytics to develop decision support systems to promote the use of renewable energy in society. Since electricity from renewable energy sources is still relatively expensive, there are variety of financial incentive programs available in different regions. Our research focuses on financial incentive programs and tackles two main problem: 1) how to optimally design and control hybrid renewable energy systems for residential and commercial buildings given the capacity based and performance based incentives, and 2) how to develop a model-based system for policy makers for designing optimal financial incentive programs to promote investment in net zero energy (NZE) buildings.

In order to customize optimal investment and operational plans for buildings, we developed a mixed integer program (MIP). The optimization model considers the load profile and specifications of the buildings, local weather data, technology specifications and pricing, electricity tariff, and most importantly, the available financial incentives to assess the financial viability of investment in renewable energy. It is shown how the MIP model can be used in developing customized incentive policy designs and controls for renewable energy system.

CHAPTER 1: INTRODUCTION

Renewable energy (RE) driven electricity generation has become a fast-growing and opportunity-rich segment of energy industry over the past few years. Since the renewable green energy generation is still relatively expensive, there are federal, state and utility incentives to increase penetration of distributed renewable energy generation. In this regards, there are two key challenges, on the investor side and on the policy makers side. For electricity consumers (buildings/investors) it is critical to investigate the financial viability of investing in on-site renewable energy systems, or otherwise keep satisfying all their energy needs from the utility companies. It is important to investigate the viability of a system that is customized for that particular building. In the other hand, policy makers has a limited budget and so it is imperative to optimally allocate budget in different types of financial incentive programs to achieve the long term goals in participation of buildings in investment in renewable energies. Such a market condition must be supported by more efficient tools providing 1) optimal design and operation services to the buildings, 2) optimal design of financial incentive programs to promote investment in renewable energies.

In the first chapter of this dissertation we have developed a decision support tool to find an optimal level of investment in a green hybrid power system (HPS), along with optimal operational strategies, to satisfy energy and reliability requirements while saving more money. Based on available incentives, consumer characteristics, technologies' specifications and local

weather data, a mixed integer program (MIP) is solved in order to find optimal design and control strategy to yield a minimum annual cost of energy. This model is particularized for wind and solar energy sources and applicable for either grid-connected or stand-alone microgrids. The financial incentive programs considered in the model are loan, rebate, performance based incentives, tax credits, renewable energy certificates, and net metering. A time-of-use (TOU) pricing structure for electricity is assumed to be in effect. Higher level of distributed renewable energy generation and storage via microgrids will lead to a significant reduction in carbon emission and also reduced cost of electricity in the grid, especially during peak times. An extended analysis has been done to examine the impact of different incentive and rebate policies within a certain budget limit on the green power generation. Thus, this MIP model may serve as a policy design aid at the local, state, and federal government levels.

Promoting net zero energy buildings (NZEB) is among the key carbon emissions reduction approaches widely adopted by policymakers in recent years in the U.S. and the EU countries [3]. Due to the relatively higher cost of electricity generation from renewable energy (RE), federal, state, and local governments offer various financial incentive programs to promote NZEB. Chapter 2 presents a model-based framework for the policymakers to design suitable incentive programs. The model in the core of this framework is the mixed integer program (MIP) that is presented in Chapter 1 of this dissertation in addition to some new constraints. The MIP model finds an optimal design for a NZEB. The optimal design and the cost of NZEB is then used to design incentive programs. The incentive programs considered

includes loans, production tax credit, and net metering, among others. A time-of-day pricing is assumed to be in effect. The model is implemented on commercial buildings in Tampa, Florida, U.S.A. For a given region, the framework provides policymakers two reports, 1) a set of optimal portfolios of incentives for different classes of commercial buildings (based on credit rating, expected return on investment (ROI), and building type), 2) for a specified portfolio of incentives, determines which classes of commercial buildings will be willing to invest in RE.

To illustrate the financial and environmental benefits of using optimization to design and operate a renewable energy system, we conducted a case study which is presented in Appendix A of this dissertation. In this case study, we aim at finding, 1) the impact of thermal energy storage (TES) on the annual energy generation in a concentrating solar powerplant (CSP), and 2) the optimal hourly operational decisions in the CSP-TES system to maximize the revenue from the output electricity to the grid. We examined this approach for the MicroCSP plant at the University of South Florida (USF). The solar field is simulated using SAM software (by NREL). The results of the simulation are fed into a Mixed Integer Linear Programming (MIP) model in order to analyze different sizing of the TES and hourly operational decisions. The results show, having at least one hours of TES capacity, significantly increases the electricity output from the power block. Moreover, an optimal operation plan increases the revenue under a time of day (TOD) price of electricity tariff.

The key input parameter to renewable energy system operation optimization model is the forecasted weather data and in particular solar energy, as solar energy production is

getting more and more popularity recently. While solar energy's advantage over fossil fuels is its positive environmental aspects, its dependency on weather condition makes it hard to confidently rely on it. In the project presented in Appendix B of this dissertation, we developed a numerical model based on GBM to predict the short term daily solar electricity generation of a set of solar farms in Oklahoma. The goal was to minimize the Mean Absolute Error (MAE) in predicting solar generation of all the locations. Our proposed model, results and some discussions are provided in the Appendix B.

CHAPTER 2: RENEWABLE ENERGY INVESTMENT AND OPERATIONAL DECISION MODEL

2.1 Introduction

Green energy industry has become a fast-growing and opportunity-rich market over the past few years globally. The U.S. market, in particular, is experiencing an increasing growth in the number of new photovoltaic capacity installations. In 2013, there was around 4.8 GW of PV installation in the U.S., which was 3.4 GW and 1.9 GW in 2012 and 2011, respectively [4]. Wind energy industry also experienced a massive growth from 2005 to 2012. New capacity installation has been for 1.1 GW, 13.1 GW, and 6.7 GW in 2013, 2012 and 2011, respectively [5]. The cost of PV system design and customer acquisition for residential PV installers was \$0.48/W in 2012. That is 9.2% of the average system price. This cost is from \$0.03/W (0.7%) to \$0.13/W (2.6%) for commercial PV systems [6]. Such a market condition must be supported by more efficient tools providing optimal design and operation services. To aid and motivate consumer communities to widely invest and participate in green power generation, we need to develop a comprehensive decision making model enabling economic capacity design and operational planning. We aim at fulfilling this need.

In this chapter, we present a mathematical model and demonstrate its use for design of on-site renewable energy system as an economically viable option for residential, commercial, or governmental buildings. The model optimizes the total cost of investment as well as

operation, and thus yields optimal operational strategies of the building with regard to their generation, storage, and trade with the grid.

Distributed renewable energy generation and storage (DREGS) will directly contribute to a number of expected benefits of smart grid, such as reduction in peak and overall electricity demand, improvements in outage management and reliability, improvements in system efficiency, and reductions in environmental emissions. To create the necessary infrastructure for microgids, power grids in the U.S. are being enhanced to enable two-way flow of electricity and information between the utilities and the consumers[7],[8].

On the other hand, there are some uncertainties in investment in renewable energies. Risks and uncertainties for PV investment have been categorized to: 1) Interannual solar variability, 2) PV performance costs, and 3) Market restructuring risk [9]. Investment in wind energy also deals with these uncertainties.

Uncontrolled variability of distributed green generation such as wind and solar are 10 % /min and 10%/s respectively. Non-renewable energy generation like coal and natural gas has rare uncontrolled variability.[10] A PV system itself has some drawbacks too, such as: 1)variation of output power with solar irradiance level causes disturbance for the utility. 2)obviously there would not be any generation during nights [11].

Considering the uncertainties in RE investment, it is very critical to decide based on all available information on incentives and regulations to ensure an acceptable payback period. We consider six main categories of incentive programs available in the U.S. such as loan program, rebate, investment tax credit, production tax credit (PTC, i.e., performance based

incentive(PBI)), renewable energy certificate (REC), and net metering. Rebate programs, federal tax credit and loan programs are incentives for installation. PTC, REC, and net metering is a production based incentive. Rebate programs that are available in some regions are intended to reduce the initial investment costs. The federal government in the U.S. is offering 30% tax credit for investment in RE and energy efficiency through Dec 31, 2016. Moreover, some states (e.g., New York) in the U.S. have their own state tax credit programs for RE investments. U.S. department of energy (DOE) provides loan guarantee for the purchase of renewable energy or energy efficient systems or equipment. PTC is a form of tax credit based on the amount of power generated by a RE system. Performance-based incentives (PBIs), provide cash based on the amount of power generated by a renewable energy system. REC is a benefit to a building based on the amount of electricity it generates from RE, and customers may sell RECs back to the utility.

In addition to the above incentive programs, we also consider in our model net metering as an incentive for buildings, when there is flow of electricity both to and from the building. We consider that the RE generation by building that exceeds its usage flows back to the grid. This offsets electricity consumed from the grid by the building. If there remains an annual rollover balance, building is paid based on the avoided cost of the local utility company. In some regions, rollover is calculated monthly and is paid at the full retail rate of electricity. Net metering is required by law in most states in the U.S. A complete list of incentive programs in the U.S. can be found in the database of state incentives for renewable energy and efficiency (DSIRE) [12].

Since the photovoltaic (PV) systems have high initial cost, they must be efficiently operated and maintained to deliver the expected benefits. This requirement serves as a barrier and pushes interested owners of residential and commercial buildings to participate in programs offered as third party ownership (TPO) solar finance companies. TPO allows the building owners to avoid the risk of investment while still reaping some of the rewards. TPO companies offer two main options: power purchase agreement (PPA) and solar lease [13]. In the PPA option, a customer is only charged upon electricity generation. In the lease option, a customer pays rent for the equipment irrespective of the amount of electricity generated. The MIP model presented in this paper can also be used by TPO companies to evaluate profitability of adding a new customer.

Current capacity designs for microgrids do not exploit incentives for green investment and generation [2], [14], [15], [16], [17], [18]. Some of the developed optimization models, design a HPS consist of both renewable and non-renewable generators[18]. Although having non-renewable generators, such as diesel, in the HPS may increase reliability of the system with a lower cost but is not a good start to move toward an environmentally responsible smart grid. The reliability issues for hybrid wind-solar system is addressable by minimizing cost within a required reliability level for the system [19]. In general a HPS can be grid-connected ([20], [18]) stand-alone ([21], [16]) or a microgrid, in a switchable mode between the two.

For an optimal operational strategy of the system, one strategy by the end user might be rescheduling flexible loads to minimize the cost[22], but this strategy only addresses the

flexible loads. The most common control strategy is optimally charge and discharge batteries, if available[11], [14], [23], [24].

Our developed MIP model will help making DREGS viable in view of economic feasibility and operating efficiency. We are developing a comprehensive and user friendly system with models at two levels. The upper level model will guide DREGS participants with economic capacity design, and the lower level model will support real-time operational planning using capacity design as input. The capacity design component of the system is a MIP model that seeks optimal capacities for generation technologies, storage batteries, inverters ,and rectifiers for the participant. The model will aim to minimize the annual cost of energy to the participant subject to the constraints of demand, weather impact on generation, technology, investment costs and incentives, and time-based rates of grid power.

For a given typical meteorological data (i.e. sunlight , ambient temperature and wind) and other energy availabilities in the region, the model will obtain an optimal capacity design incorporating the number and types of green generators, converters and power storage facilities. Thereafter, for a given capacity design, the operational planning model will take into account the daily weather forecast, time-based rates of the grid, and the demand response guidelines, to optimize real-time operational plan. The plan would comprise optimal rates for battery charging/discharging, demand response actions, and optimal quantities of power bought from and sold back to the grid under net-metering policy.

We believe that our system, with CPLEX implementable solution strategies for its underlying models, will empower households and businesses across the world, with or without

smart grid infrastructure, to assess potential to build and operate a green HPS. Expected proliferation of DREGS, assisted by our system, would allow an increased realization of the broad range of benefits of smart grid. We have already developed a single investor model for capacity design and operation control, which is presented later in this document.

2.2 Problem Statement

In building a design and control optimization model, there are multiple issues that are important to address. Some regarding to the physical system components, such as the generators, batteries and converters. Other considerations pertain to the regulations and economic aspects of the design and operation. In this section we go over these aspects and how we address them in the model. Solar and wind energy are the most popular renewable energy sources and we are focusing on these sources for the design of the hybrid system.

The orientation of the photovoltaic (PV) panel determines the incidence angle of the solar radiation and the resulting output power. The literature provides that a general optimum tilt of the solar panel is a slope close to the latitude and orientation toward south/north for northern/southern hemisphere [25]. The conversion efficiency of PV system decreases as module temperature goes higher. For example, the temperature coefficient of heteromodule, c-Si module, and p-Si module was $-0.3\%/\,^{\circ}\mathrm{C}$,$-0.4\%/\,^{\circ}\mathrm{C}$,and$-0.4\%/\,^{\circ}\mathrm{C}$, respectively [26]. We considered the tilt angle and the variable efficiency of PV in the section 2.3.2.

Wind generator's power output depends on the local wind speed profile. Also wind generators have different power output performance curves. The most common model to simulate wind energy generation is a non-linear model. So we simulate the wind profile in a

data pre-processing phase and before the MIP model (look section 2.3.2). Also, the height of the wind turbine can largely effect the wind speed profile[27], so we considered the option of selecting height of the wind turbine by type of installation in the MIP model.

Battery storage is used as a backup to meet the demand and hedge against the renewable energy volatility. It is highly crucial for a stand-alone microgrid to be supported by storages, specially for night hours that it may only have the wind energy as a source of power and even may not. For a grid-connected microgrid, energy storage can increase reliability of the system when the grid power is not available for any reason. Selecting the right size for the battery to meet the required reliability is an economic imperative. Battery's lifetime is much shorter than generator so it needs replacement multiple time during the system lifetime.

Connecting the solar and wind generators along with storages to the grid requires appropriate conversions. It is technically feasible to use only one inverter to connect both storages and the PV array to the AC node [11]. The size/number of inverters need to satisfy the system requirements and also be cost effective.

In a restructured electricity market, generators submit bids to the system operator and the clearing price for electricity will be established[28]. However as a single member microgrid, we assumed the generator is not an active bidder and price is based on net-metering with local utility.

This chapter presents a mixed integer programming (MIP) model that determines for microgrids (buildings) the optimal levels of investment in renewable energy technology

including wind and solar generators, converters and storage capacities. The model assumes that a number of incentive programs are in place, including lower loan interest rate, rebate, PTC, REC, net metering, and time-of-use (TOU) pricing. The MIP minimizes the total cost of meeting the energy needs over a planning horizon by minimizing the average annual cost. The cost minimization approach also yields an optimal operational strategy for electricity storage and trade with the grid. The objective function comprises the cost of capital, cost of operation and maintenance, net metered electricity bill, tax credits, rebates, PTC, and REC. The MIP model offers the ability to conduct sensitivity analysis for a wide range of variables related to incentive programs, technology, weather, and grid electricity prices. We have presented, in a later section, results from such a sensitivity analysis on the incentive program parameters and electricity rate structure.

To our knowledge, our model is new as it offers a means for evaluating the impact of a wide array of incentive programs. From several aspect of our modeling approach, here some of them are highlighted: 1) it considers incentive programs offered by federal, state, and local agencies, 2) it considers the option to buy from or sell back to the grid at hourly prices (TOU price of electricity), 3) it takes into account equipment maintenance schedules and weather changes, and 4) it yields both the capacity investment decision and the corresponding operational strategy.

2.3 Model Formulation

In this section we introduce the nomenclature and the mathematical model.

2.3.1 Nomenclature

The notation used for the model is presented in Table 1.

Table 1: Nomenclature used in chapters 2 and 3

Symbol	Meaning
Indices	
k	Types of RE generators (k^1 for AC and k^2 for DC, where $\{k\} = \{k^1\} \cup \{k^2\}$)
p	Types of converter (= 1 for inverter, = 2 for rectifier)
ℓ	Types of generator installation (e.g., height of wind turbine tower, roof or ground mount solar panels)
n	Age of the RE power system in years, $n \in \{1, \ldots, N\}$
t	Hour of the year, $t \in \{0, \ldots, 8760\}$
Decision Variables	
$x_G^{k\ell}$	$\in \mathbb{Z}^+$, Number of generators of type $k\ell$
x_B	$\in \mathbb{Z}^+$, Number of energy storages (battery)
x_C^p	$\in \mathbb{Z}^+$, Number of converters of type p
q^t	$\in \mathbb{R}$, Electricity trade with the grid at t (Wh)
Calculated Variables	
w	$\in \mathbb{R}$, Annual net metering credit (\$)
u	$\in \mathbb{R}^+$, Loan amount used for investment in RE (\$)
r^k	$\in \mathbb{R}^+$, Rebate received for investment in type k (\$)
a^k	$\in \mathbb{R}^+$, State tax credit for type k (\$)
h	$\in \mathbb{R}^+$, Annual electricity bill (\$)
$g^{k\ell t}$	$\in \mathbb{R}^+$, Total power output of generators k, ℓ at t (Wh)
e_1^t	$\in \mathbb{R}^+$, DC Power sent to battery at t (Wh)
e_2^t	$\in \mathbb{R}^+$, AC Power sent to battery at t (Wh)
e_3^t	$\in \mathbb{R}^+$, Power received from battery at t (Wh)
z^t	$\in \mathbb{R}^+$, Power level of battery at t (Wh)
μ^t	$\in \{0, 1\}$, 1 if batteries are being charged at t
$y_G^{k\ell}$	$\in \{0, 1\}$, 1 if invested in generators type $k\ell$
y_B	$\in \{0, 1\}$, 1 if invested in batteries
Incentive Parameters	
γ_F	The federal tax credit rate for RE (%)
γ_s^k	The state tax credit rate for generator k (%)
$\overline{a}^k$	State tax credit cap for generator k (\$)

Table 1 (continued)

Symbol	Meaning
J	Customer renewable energy certificates (REC)($)
I^k	PTC rate for generator k ($/Wh$)
R^k	Rebate for investment in generator k, for solar energy ($/W$) and for wind energy ($/kWh$)
$\overline{R}^k$	Rebate cap for investing in generator k ($)
α	Interest rate for loan program (%)
n_u	Loan term for RE installation ($years$)
$\overline{U}_1^k$	Loan cap for investing in generator k, ($)
$\overline{U}_2$	Loan cap proportional to the total investment (%)
λ	Local utility's annual rollover compensation,($)
Input Parameters	
β	Annual discount rate (the value of money) (%)
β'	Hourly discount rate ($= \sqrt[8760]{1+\beta} - 1$) (%)
H^t	Grid electricity price at t ($/Wh$)
h_0	Annual basic service charge on grid electricity ($)
h_1	Peak billing demand on grid electricity ($)
h_2	Billing demand on grid electricity ($)
$F_G^{k\ell}$	Fixed cost of investment in generator type $k\ell$ ($)
$V_G^{k\ell}$	Variable cost of investment in generator type $k\ell$ ($/W$)
F_B	Fixed base cost of investment in battery ($)
V_B	Variable cost of investment in battery ($/W$)
C_C^p	Purchase cost of converter type p ($/W$)
ψ	Operation and maintenance costs coefficient (%)
$\Gamma_G^{k\ell}$	Nominal capacity of generator type k, ℓ (W)
Γ_C^p	Power input capacity of converter type p (W)
Γ_B	Nominal capacity of battery (Wh)
N	Expected lifetime of the hybrid power system, ($years$)
n_B	Expected lifetime of battery, ($years$)
n_C^p	Expected lifetime of converter type p, ($years$)
GHI^t	Global horizontal solar irradiance at t (W/m^2)
E^t	Module solar irradiance at t (W/m^2)
ν^{tl}	Wind speed installed at height ℓ at t (m/sec)
ν_{ci}	Cut-in wind speed (m/sec)
ν_{co}	Cut-out wind speed (m/sec)
ν_r	Wind speed at the rated power (m/sec)
$\omega^{k\ell t}$	Output power of a generator type $k\ell$ at t (Wh)
G_{max}	A big number relative to the total generation (W)
B_{max}	A big number relative to the total storage (Wh)
ϵ_1	Charging efficiency rate of battery (%)
ϵ_2	Discharging efficiency rate of battery (%)

Table 1 (continued)

Symbol	Meaning
θ_1	Nominal charging rate of battery (%)
θ_2	Nominal discharging rate of battery (%)
ϕ_1	Hourly decay rate in charge level in battery (%)
ϕ_2	Min. sustainable charge level ratio in battery (%)
η_p	The efficiency rate of the converter p (%)
$\eta^{k\ell t}$	The efficiency rate of generator $k\ell$ at t (%)
η_R^k	Reference efficiency rate of generator k (%)
ζ^k	Temperature coefficient of generator k ($/^\circ C$)
$T^{t\ell}$	Temperature at t around ℓ ($^\circ C$)
T_R	Temperature at reference conditions,($^\circ C$)
D_{AC}^t	Demanded AC load at t (kWh)
D_{DC}^t	Demanded DC load at t (kWh)
Δ	Load reduction ratio through efficiency improvement
D_1^t	Billing demand at t (kWh)
D_2	Peak billing demand (kWh)
M	Minimum power supply (reliability) ($hour$)
$A^{k\ell}$	Area occupied by generator $k\ell$ (m^2)
$\overline{A}^{k\ell}$	Total available area for installation ℓ of k (m^2)
L_{DC}	Derate factor for DC wiring (%)
L_{AC}	Derate factor for AC wiring (%)
L_M^k	Derate factor for mismatch of generator type k (%)
L_R^k	Derate factor for nameplate DC rating of type k (%)
L_S^k	Derate factor for soiling of PV ($k = 1$) (%)
L_V^k	Derate factor for system availability of type k (%)
L_D^k	Derate factor for shading of PV ($k = 1$) (%)
L_A^k	Derate factor for age/degradation of PV ($k = 1$) (%)
L_C^k	Derate factor for diodes and connections (%)
L_T^k	Derate factor for sun-tracking of PV ($k = 1$) (%)

2.3.2 Other Model Preliminaries

In order to make the input data ready for the MIP model the following data pre-processing steps have been performed.

- PV module ($k = 1$) efficiency is calculated as a function of the operating temperature as follows [29]: $\eta^{k\ell t} = \eta_R^k - \zeta^k(T^{t\ell} - T_R)$.

- Solar radiation incident on a PV module surface, tilted by ρ° at latitude σ°, is calculated by $E^t = \frac{GHI^t \sin(\upsilon+\rho)}{\sin(\upsilon)}$, where $\upsilon = 90^\circ - \sigma + \delta$, and δ, the solar declination, equals $23.45^\circ + \sin(\frac{360}{365}(284 + day))$ [30].
- PV ($k = 1$) output power (DC) is calculated based on the hourly efficiency of solar installation ℓ as follows: $\omega^{k\ell t} = \eta^{k\ell t} E^t A^{k\ell} L_M^k L_R^k L_S^k L_D^k L_A^k L_C^k L_T^k, \ \forall \ell, t$
- Output power of the wind turbine has a non linear relation to the wind speed.

$$\omega^{k\ell t} = \begin{cases} a(\nu^{t\ell})^3 - b\Gamma_G^{k\ell} & \nu_{ci} \leq \nu^{t\ell} \leq \nu_r, \\ \Gamma_G^{k\ell} & \nu_r \leq \nu^{t\ell} \leq \nu_{co}, \\ 0 & \text{o/w}, \end{cases}$$

where $a = \frac{\Gamma_G^{k\ell}}{\nu_r^3 - \nu_{ci}^3}$ and $b = \frac{\nu_{ci}^3}{\nu_r^3 - \nu_{ci}^3}$, $\forall i, t$.

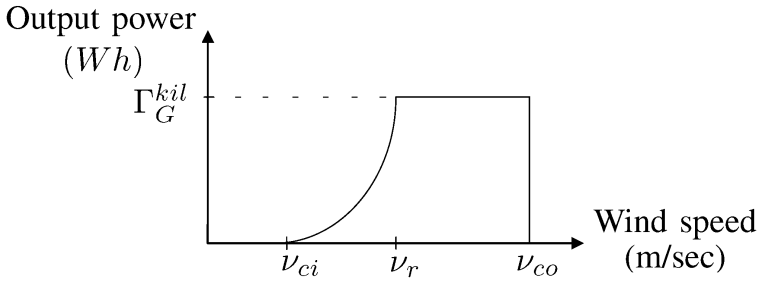

Figure 1: Output power versus wind speed [2]

2.3.3 MIP Model

We have developed a Mixed Integer Programming (MIP) model and solved using CPLEX solver in GAMS. The goal is to find optimal level of investment and optimal control strategies to yield a minimum annual cost of energy. Here we presented the objective

function and constraints of the MIP model for both investment and operational decisions. The investment MIP model is able to find the optimal system design for two modes of the microgrid, grid-connected and stand-alone modes. These models will be presented in the following sections.

2.3.3.1 Investment Model (System Design) for Design of a Grid-Connected HPS

For a grid-connected mode, we assumed the microgrid is under a net-metering policy. The system components for a grid-connected microgrid are shown in Figure 2.

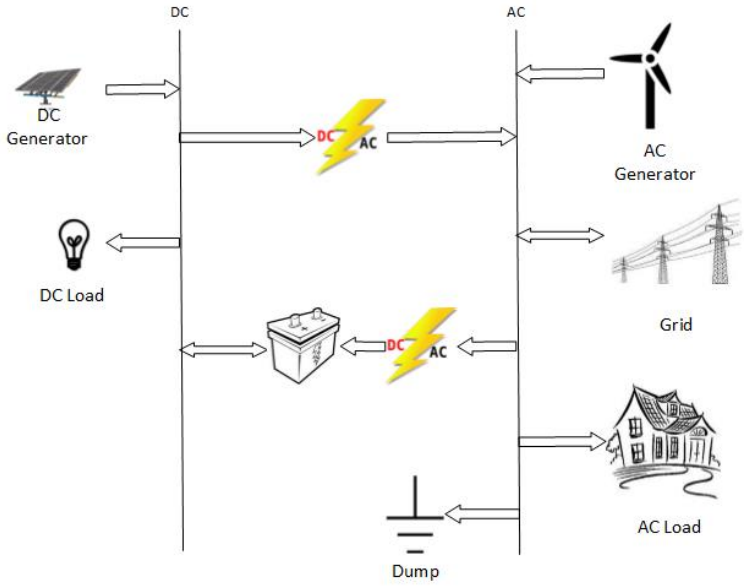

Figure 2: Design of the DC/AC for a grid-connected HPS

$$min\, Z = [\frac{n_u}{N}(\frac{\alpha u}{1-\frac{1}{(1+\alpha)^{n_u}}}) + \frac{\beta\frac{N}{n_B}(y_B F_B + x_B \Gamma_B V_B)}{1-\frac{1}{(1+\beta)^N}}$$
$$+\frac{\beta(\sum_k[\sum_\ell(y_G^{k\ell}F_G^{k\ell} + x_G^{k\ell}\Gamma_G^{k\ell}V_G^{k\ell}) - r^k] - u)}{1-\frac{1}{(1+\beta)^N}}$$

$$+\frac{\beta\sum_p \frac{N}{n_C^p} C_C^p x_C^p \Gamma_C^p}{1-\frac{1}{(1+\beta)^N}} + \psi\{(y_B F_B + x_B \Gamma_B V_B) + \sum_{k\ell}(y_G^{k\ell} F_G^{k\ell} + x_G^{k\ell}\Gamma_G^{k\ell} V_G^{k\ell}) + \sum_p C_C^p x_C^p \Gamma_C^p\}$$

$$-\sum_k a^k - \gamma_F \frac{1}{N}\frac{N}{n_B}(y_B F_B + x_B \Gamma_B V_B) - \gamma_F \frac{1}{N}\sum_k (\sum_\ell (y_G^{k\ell} F_G^{k\ell} + x_G^{k\ell}\Gamma_G^{k\ell} V_G^{k\ell}) - r^k)$$

$$-\gamma_F \frac{1}{N}\sum_p \frac{N}{n_C^p} C_C^p x_C^p \Gamma_C^p]/(1+\beta)$$

$$+\frac{12\{D_1 h_1 + \frac{\sum_t D_2^t}{8760} h_2\}}{1+\frac{\beta}{2}} + \frac{h_0 + h + \lambda w}{1+\frac{\beta}{2}} - \sum_t \frac{\sum_k I^k \sum_\ell g^{k\ell t}}{(1+\beta')^t} - \sum_t \frac{J\sum_{k\ell} g^{k\ell t}}{(1+\beta')^t} \tag{2.1}$$

$$g^{k\ell t} = \omega^{k\ell t} x_G^{k\ell} L_V^k \ \forall k, \ell, t \tag{2.2}$$

$$x_G^{k\ell} \leq y_G^{k\ell} G_{max} \ \forall k, \ell \tag{2.3}$$

$$x_B \leq y_B B_{max} \tag{2.4}$$

$$\epsilon_1(e_1^t + e_2^t) \leq x_B \Gamma_B \theta_1 \ \forall t \tag{2.5}$$

$$e_1^t + e_2^t \leq \mu^t B_{max} \forall t \tag{2.6}$$

$$\epsilon_2^{-1} e_3^t \leq x_B \Gamma_B \theta_2 \forall t \tag{2.7}$$

$$e_3^t \leq (1-\mu^t) B_{max} \forall t \tag{2.8}$$

$$\eta_1[\sum_{k^1\ell} g^{k^1\ell t} + (e_3^t - e_1^t)] L_{DC} L_{AC} - \eta_1(1-\Delta) D_{DC}^t L_{DC}$$

$$+\sum_{k^2\ell} g^{k^2\ell t} L_{AC} + q^t = (1-\Delta) D_{AC}^t + \frac{1}{\eta_2} e_2^t \qquad \forall t \tag{2.9}$$

$$z^t = x_B \Gamma_B \forall l, t = 1 \tag{2.10}$$

$$z^t = (1-\phi_1) z^{(t-1)} - \epsilon_2^{-1} e_3^t + \epsilon_1(e_1^t + e_2^t) \forall t \geq 2 \tag{2.11}$$

$$z^t \geq \phi_2 x_B \Gamma_B \forall t \tag{2.12}$$

$$z^t \leq x_B \Gamma_B \forall t \tag{2.13}$$

$$\sum_{k\ell} g^{k\ell t} + (e_3^t - e_1^t) - (1-\Delta)D_{DC}^t \leq x_C^p \Gamma_C^p \forall t, p = 1, k \in k^1 \tag{2.14}$$

$$\frac{1}{\eta_2} e_2^t \leq x_C^p \Gamma_C^p \forall t, p = 2 \tag{2.15}$$

$$D_2^t \geq q^t \ \forall t \tag{2.16}$$

$$D_1 \geq D_2^t \ \forall t \tag{2.17}$$

$$h \geq \sum_t q^t H^t \tag{2.18}$$

$$w = \sum_t q^t H^t - h \tag{2.19}$$

$$\sum_{k\ell} \sum_{t'=t}^{t+M} g^{k\ell t'} + z^t \geq \sum_{t'=t}^{t+M} (1-\Delta)(D_{AC}^{t'} + D_{DC}^{t'}) \forall t \tag{2.20}$$

$$A^{k\ell} x_G^{k\ell} \leq \overline{A}^{k\ell} \ \forall \ell, k = 1 \tag{2.21}$$

$$A^{k\ell} y_G^{k\ell} \leq \overline{A}^{k\ell} \forall \ell, k = 2 \tag{2.22}$$

$$\sum_{\ell} y_G^{k\ell} \leq 1 \ k = 2 \tag{2.23}$$

$$r^k \leq R^k \sum_{\ell} x_G^{k\ell} \Gamma_G^{k\ell} k = 1 \tag{2.24}$$

$$r^k \leq R^k \sum_{\ell t} g^{k\ell t} k = 2 \tag{2.25}$$

$$r^k \leq \overline{R}^k \ \forall k \tag{2.26}$$

$$u \leq \overline{U}_2 [\sum_p x_c^p C_C^p \Gamma_C^p + x_B V_B \Gamma_B + y_B F_B + \sum_k (\sum_{\ell} [y_G^{k\ell} F_G^{k\ell} + x_G^{k\ell} \Gamma_G^{k\ell} V_G^{k\ell}] - r^k)] \ \forall k \tag{2.27}$$

$$u \leq \overline{U}_1^k \ \forall k \tag{2.28}$$

$$a^k \leq \gamma_s^k \sum_{\ell} (y_G^{k\ell} F_G^{k\ell} + x_G^{k\ell} \Gamma_G^{k\ell} V_G^{k\ell}) \ \forall k \tag{2.29}$$

$$a^k \leq \overline{a}^k \ \forall k \tag{2.30}$$

$$x_G^{k\ell}, x_C^p, x_B \in \mathbb{Z}^+ \cup \{0\},\ q^t, w \in \mathbb{R},\ y_G^{k\ell}, y_B, \mu^t \in \mathbb{B}$$

$$g^{k\ell t}, u, r^k, z^t, e^t, D_1, D_2^t h, a^k \in \mathbb{R}^+ \cup \{0\} \tag{2.31}$$

The investment and financing time horizon considered in the model are 30 years. All capital costs and credits are depreciated over 30 years in addition to other annual costs and revenues. We annualized all costs and revenues in the MIP model in the objective function, aiming at minimization of the overall cost of electricity in a building for a typical year.

The positive elements of the objective function (2.1) represent equivalent annual cost and the negative elements indicate yearly revenue or credits. The seven cost elements indicate, in order presented in (2.1), the loan annual payment, depreciated annual cost of capital used for technology procurement and installation (including fixed and variable costs of batteries, generators, and converters), annual operation and maintenance costs, and billing demand and peak billing demand charges. The last positive element of the objective function represents the basic service charge of the utility company in addition to the cost of net electricity purchase from utility (when $h \geq 0$) or revenue from annual rollover compensation (when $\omega < 0$). The revenue/credits comprise rebates, state tax credit, federal tax credit for capital investment (in batteries, generators, and converters), the production tax credit (PTC), and renewable energy certificate (REC).

The constraints are as follows. Constraint (2.2) calculates electricity generation by each type of generator based on the corresponding weather data and the derate factor of availability. Constraints (2.3,2.4) are to include fixed cost associated with the installation of

the system, i.e., if $x_G^{k\ell}$ takes a positive value, the inequality forces $y_G^{k\ell}$ to take one as well, and similar for y_B. Constraints (2.5) and (2.6) show the rate of charge of the batteries considering charging efficiency and nominal charging rate. Constraints (2.7) and (2.8) show the rate of discharge of the batteries considering discharging efficiency and nominal discharging rate. In (2.6) and (2.8), μ^t ensures that a battery is not charged and discharged at the same time t. Balance constraint (2.9) ensures that the energy input to a microgrid equals its output, both for DC and AC, at all times. Constraints (2.10) through (2.13) accomplish hourly updates of the battery capacities. Power conversion from DC to AC and vice versa is always limited by the capacities of inverters (2.14) and rectifiers (2.15). It is considered that the utility gives credit to the microgrids for selling electricity back to the grid. As practiced by many states in the U.S., if total yearly sales credit exceeds total purchase of a building, the utility pays for the excess credits to the consumer. The constraints (2.16) and (2.17) calculates annual peak and base demand of the building for electricity from the grid. The constraints (2.18) and (2.19) calculate annual electricity payment to the utility company, if any, and sales credits, respectively. To ensure that the customer has power during blackouts for at least M hours (reliability), we added constraint (2.20) to the model. The installation capacity limits for generating devices are handled by (2.21) through (2.23). Constraints (2.24) through (2.30) accounts for the rebate, loan, and state tax credit amounts resulting from the investment plan.

2.3.3.2 Investment Model (System Design) for Design of an Stand-alone HPS

The system components for an stand-alone microgrid are shown in Figure 3. Basically, the same MIP model can be used to design an stand-alone (not connected to the main grid) HPS with some modifications. To enforce the system to run independently without the grid, we need to add the following constraint: $q^t = 0 \ \forall t$ Since the system might have amount of not needed power; now s^t,the dumped power, may get positive values for some t times.

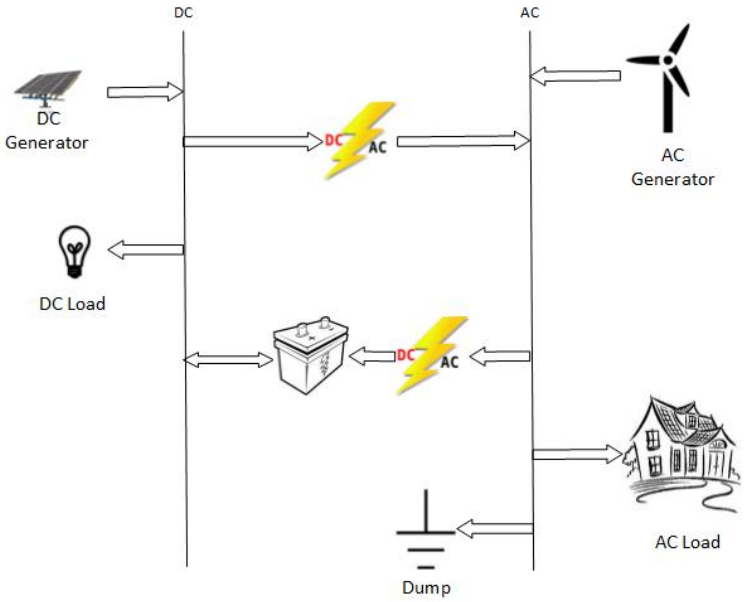

Figure 3: Design of the DC/AC for a stand-alone HPS

2.3.3.3 Operational Model (System Control)

For a stand-alone HPS, the only way that the user can optimize the energy efficiency is by scheduling flexible power load [22], which requires a separate optimization modeling. In grid-connected mode, the Operational model takes $x^{kil}_{GEN}, x^{j}_{BAT}, x^{j}_{CNV}$ as input parameters along with other inputs and this time decision variables is q^t. This model assumes a net-metering policy in the grid.

$$min \ \frac{12\{D_1 h_1 + \frac{\sum_t D_2^t}{8760} h_2\}}{1+\frac{\beta}{2}} + \frac{h_0 + h + \lambda w}{1+\frac{\beta}{2}} - \sum_t \frac{\sum_k I^k \sum_\ell g^{k\ell t}}{(1+\beta')^t} - \sum_t \frac{J \sum_{k\ell} g^{k\ell t}}{(1+\beta')^t} \quad (2.32)$$

$$s.t. \ \{(2.2) - (2.20)\}$$

2.4 Model Implementation

We tested the renewable energy investment and operational planning MIP model for two residential buildings in the U.S., in different climates, one in Tampa, FL, and the other one in Long Island, NY. We provide the input data, and show the results of the MIP model for optimal investments and operations of the buildings. Later in this section, we illustrate our observations on sensitivity analysis of the investment level in renewable energy in the studied building in Tampa, Fl, with respect to different incentive programs.

2.4.1 Data

2.4.1.1 Customer Data

The customer characteristics used in the MIP model are 1) building characteristics, and 2) residential hourly load data. The above data were obtained from "Building America House Simulation Protocols-NREL [31]." Based on this protocol, the residential buildings are classified as one of the following categories: 1) low load profile, 2) base load profile, and 3) high load profile. Residential load profile and building characteristics for a hot-humid and mixed-humid climates were used for Tampa, Fl, and Long Island, NY, respectively. The size of the buildings for different load profiles and climates are given in Table 2.

Table 2: Residential load profiles

Load profile	Size, mixed-humid	Size, hot-humid
Low Load (LL)	$1273ft^2(118.3m^2)$	$1011ft^2(93.9m^2)$
Base Load (BL)	$2546ft^2(236.5m^2)$	$2023ft^2(187.9m^2)$
High Load (HL)	$3819ft^2(354.8m^2)$	$3034ft^2(281.9m^2)$

A summary of a typical customer's characteristics for a low load profile electricity consumer is provided in Table 3.

Table 3: The low load profile customer characteristics

PV area (mixed-humid)	$118.3m^2$ ($1273ft^2$) roof area for PV installation
PV area (hot-humid)	$93.9m^2$ ($1011ft^2$) roof area for PV installation
Wind area	$50m^2$ ($538.2ft^2$) available for wind turbines
Demand	hourly demand data from OpenEi.org [32]
Beta	5 % (personal fund ROI)

2.4.1.2 Incentives/Regulations

In Table 4, we have listed all currently available incentives and regulations for residential customers for renewable energy installations in Tampa, FL. Table 5 contains similar data for Long Island, NY.

Table 4: Incentive and regulations in Tampa, Fl

Tax credit	30% of total investment
TOU price	On-peak: 18.436 (¢/kWh)
	Off-peak: 5.698 (¢/kWh)
Peak hours	Nov-Mar (Winter) : 6:00AM-10:00AM
	: 6:00PM-10:00PM
	Apr-Oct (Summer) : Noon-9:00PM

2.4.1.3 Technology Options

We have considered four different models ($i = 1, .., 4$) of PV solar panels ($k = 1$) to be available in the market. The representative cost of each PV model (obtained from [33])

Table 5: Incentive and regulations in Long Island, NY

Federal tax credit	30% of total investment
State tax credit	25% of PV investment up to $5000
Wind rebate	Rebate = Min{60% of installed cost, $3.50 per expected kWh}
	Max rebate = Min{60% of installed cost, $56,000}
	Max size = Min{105% prior 12 months energy usage, 25 kW}
PV rebate	Rebate = $1.00/W
	Max size = Min{25 kW, 110% of energy usage}
TOU price	
Jun-Sep	On-peak: 27.35 (¢/kWh)
	Off-peak: 5.78 (¢/kWh)
Oct-May	On-peak: 8.88 (¢/kWh)
	Off-peak: 4.37 (¢/kWh)
On-peak hours	10 AM-8 PM Weekdays
Off-peak hours	8 PM-10 AM Weekdays and all day weekends

also includes cost of the required racking and wirings. We have assumed the PV panels are installed at a tilt angle almost equal to the latitude of the location (28 degrees for Tampa and 41 degrees for Long Island). Table 6 shows the solar panel model options.

Table 6: Representative solar panel models

Model	**Price**($)	**Capacity (W)**	**Efficiency (%)**	**Size** m^2
PV1	285	274.5	0.157	1.944
PV2	339	243	0.161	1.593
PV3	171	171	0.149	1.277
PV4	295	247.5	0.164	1.593

Also, our MIP implementation considered three models ($i = 1, 2, 3$) of wind turbines ($k = 2$). The cost of each model includes the costs of mount and wirings. Table 7 shows some of the wind turbine technology options for the customer.

Table 7: Representative models for small wind turbines

Model	**Price** (\$)	**Rated Power** (W) **at 12** (m/s)	**Cut in** (m/s)	**Cut out** (m/s)
W1	419	600	2.5	15
W2	300	400	3.0	25
W3	355	600	3.0	15
W1	225	300	2.5	18

We also considered four different models of batteries (Table 8) and five models of inverters (Table 9).

Table 8: Representative models for batteries

Model	**Price** (\$)	**Capacity** (Wh)	**Size** m^2
B1	96	600	0.03
B2	370	2400	0.108
B3	223	1320	0.057
B4	64	420	0.026

Table 9: Representative models for inverters

Model	**Price**(\$)	**Input Cap(W)**	**Output Cap(W)**	**Efficiency**(%)
INV1	1485	3200	3000	96
INV2	205	250	240	96
INV3	1869	4750	3800	96
INV4	164	300	250	96
INV5	150	265	250	96

2.4.1.4 Local Weather Data

The hourly historical data on solar radiation and wind speed level for the two areas (Tampa and Long Island) are imported from the System Advisor Model (SAM) software [34].

2.4.2 Results

We used CPLEX to solve the MIP model on a standard desktop computer with 16 GB RAM and Intel i7 processor @2.93 GHz. The station took 112 and 244 seconds, to solve each load scenario for Tampa and Long Island, respectively. The solution gap was set to 0.5%.

2.4.2.1 Residential Building in Tampa, Fl

For a low load profile residential building in Tampa, Fl, the MIP model produced the following results. The proposed investment decision are:

- $x_G^{13} = 73$ (solar panels of model type 3)
- $x_C^{11} = 1$ and $x_C^{13} = 2$ (inverters of model types 1 and 3).

The proposed operational plan is that, with no batteries per investment decision, to consume electricity from solar panels, when needed, and sell any excess to the grid (similar to Figure 5). Investment and its operational plan yielded the following benefits for the building.

- Annual electricity cost reduced to $ 1420 compared to the current electricity bill of $ 1550
- Annual generation of 22.65 MWh green energy, which is equivalent to about 15.6 MT/yr (34,400 lbs/yr) reduction of carbon emissions and the building is now a NZEB.
- Total tax credits received is equal to $6878

2.4.2.2 Residential Building in Long Island, NY

For a low load profile residential building in Long Island, NY, results obtained by the MIP model are as follows. The proposed investment decision are:

- $x_G^{11} = 1$ (solar panels of model type 1)

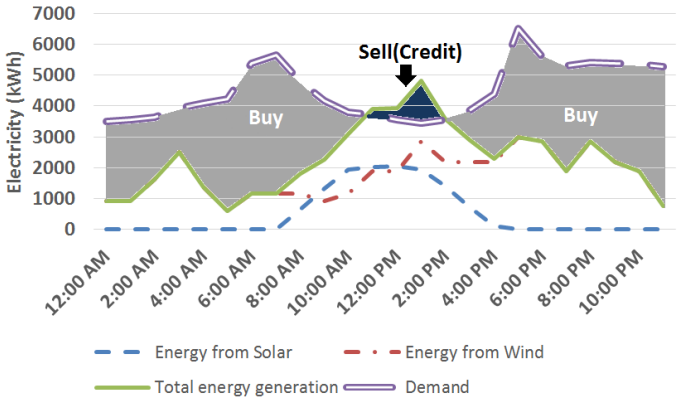

Figure 4: 24 hours of net metering in January for the NZEB in Long Island, NY.

- $x_G^{13} = 26$ (solar panels of model type 3)
- $x_G^{23} = 5$ (wind turbine of model type 3)
- $x_C^{13} = 1$ (inverters of model types 3).

Again with no batteries chosen by the investment plan, typical 24 hours operational plans are shown for the designed NZEB (with hybrid system of wind and solar) are shown for the months of January (Figure 4) and July (Figure 5). The above investment and its operational plan yielded the following benefits for the building.

- Annual electricity cost reduced to $394 compared to the current utility bill of $892.
- Annual generation of 7.2 MWh from solar energy and 1.9 MWh from wind energy, equivalent to a reduction of 6.3 MT/yr (13,900 lbs/yr) of carbon and the building is now a NZEB.
- Federal Tax Credit : $1124
- NY State Solar Tax Credit: $1183
- Wind energy rebate: $1775
- Solar energy rebate: $4720

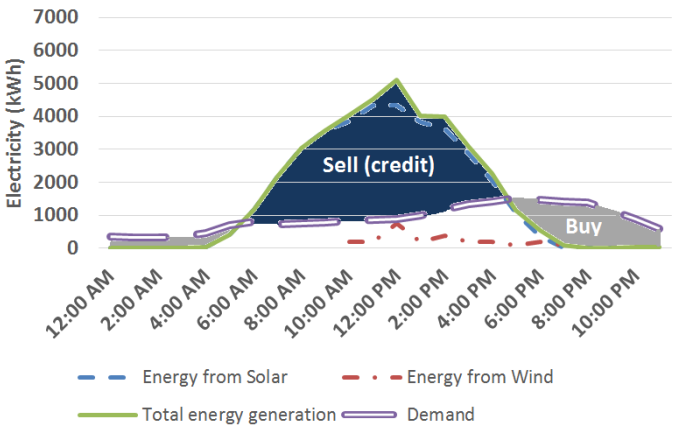

Figure 5: 24 hours of net metering in July for the NZEB in Long Island, NY.

2.4.3 Sensitivity Analysis

In the rest of this chapter we demonstrate how the MIP model can be used to understand investors' (building owners) behaviour in response to changes in the available incentives in Tampa, FL. To examine the impact of change in incentive programs on different residential customers, the sensitivity analysis was conducted for customers (buildings) with low, base, and high load profiles. As PBI, TOU pricing structure, and rollover compensation, in most areas in the U.S., are directly administrated by the local utilities commissions [12], several combinations of these incentive programs have been examined.

2.4.3.1 Effect of Loan Interest Rate

The optimal investment levels in renewable energy based generation for different loan APR are shown in Figure 6. We assumed PBI of 0, time of use (TOU) price of electricity, and return on investment (ROI) of 5%. Results show that for the given technology, cost, and weather conditions, the APR of up to 1.4% makes it economically feasible to invest in renewable (solar) energy for residential customers with different load profiles in Tampa area.

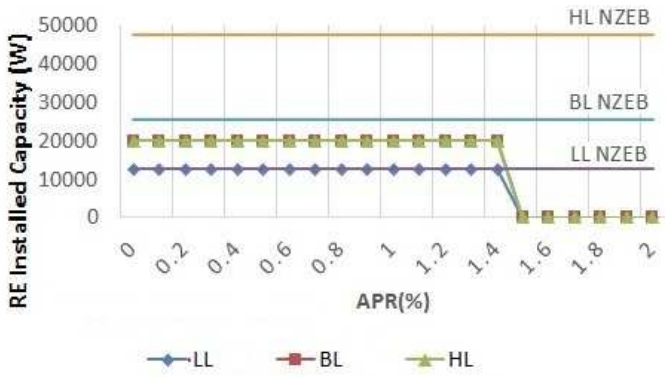

Figure 6: Sensitivity of renewable energy investment to the loan interest rate - under TOU price of electricity and PBI=0

Note that since the APR threshold for each type of energy source should be guided by its levelized cost of electricity (LCOE) generation, it is independent of the customer load profile. The APR threshold for investment depends on the green energy source availability, price of technology, other incentives and regulations. As shown in Figure 6, the level of investment depends on the load profile and the loan cap (which in this study is taken as \$20K). An interesting observations that we made in the sensitivity analysis was if the loan cap is high enough, the optimal investment level in renewable energy may rise to the net zero energy level (NZE/NZEB level). NZE level is the level of annual generated on-site electricity where it satisfies the load and the losses in the system under a net metering policy. In this analysis at such point, the annual electricity bill or rollover credit is close to zero. (see, for example, the low load level). For BL and HL levels, loan cap keeps the RE investment lower than NZEB levels.

2.4.3.2 Effect of Performance Based Incentive (PBI)

For different PBI rates, optimal investment levels in renewable energy based generation are presented in Figure 7. We assumed TOU price of electricity, no loan, and 5% ROI for the

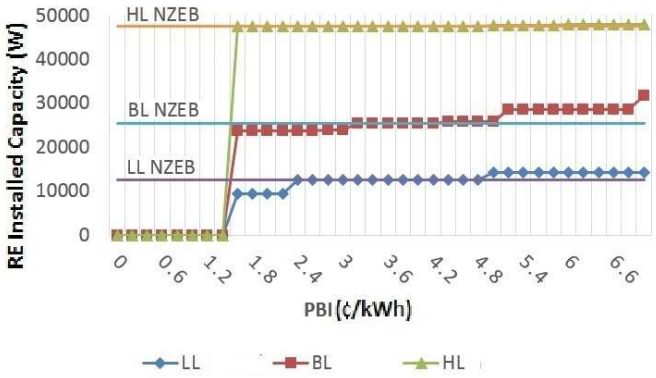

Figure 7: Sensitivity of renewable energy investment to PBI - under TOU price of electricity and self fund interest rate of 5%

investors. Note that the area available for PV deployment could become a limiting factor for solar installed capacity. Results show that a PBI rate of 1.6 ¢/kWh or more makes it feasible for residential customers (in Tampa, Fl) with different load profiles to invest in RE. Similar to analysis on loan, as demonstrated in Figure 7, customers with all load profiles reached their full NZE levels at different PBI values. Investment levels can be seen to change in steps at different PBI values. This can be attributed to the integer optimal solutions of the MIP model for all system components. At PBI of 5.2 ¢/kWh or more, buildings are found to invest in more than their net zero needs, as it is profitable (see low and base loads in Figure 7). The customer with high load profile, was found to be constrained by the available area for PV deployment and thus could not invest beyond NZE level. At present, there is no PBI in Tampa area, but in the closest city (with similar climate conditions), Orlando, the utilities commission (OUC) pays a PBI of 5 ¢/kWh [12]. This rate is clearly (see Figure 7) in the range that encourages RE investments.

2.4.3.3 Joint Effect of TOU Price and PBI

Effect of different TOU pricing schemes were examined for some PBI levels. Knowing that under current TOU tariff, a minimum PBI of 1.6 ¢/kWh is necessary to encourages investment in RE, three PBI levels (0, 1.5, 3.0 ¢/kWh) were studied. TOU pricing schemes given in Table 10 were designed such that for a base load profile (BL) the annual bill for electricity is constant for all off-peak and on-peak price combination. This helped us to assess the effect of TOU pricing scheme on the investment behaviour without any influence from the varying cost of buying electricity from the grid. We assumed a ratio of 0.3 for rollover compensation to retail price in net metering, as it was the prevailing value in 2013 in Tampa, Fl. We also assumed that no loan is available and the ROI for the investors is 5%.

When PBI is 0, Figure 8 shows no investment in RE except at a standard flat rate of electricity (i.e., off-peak/on-peak price ratio = 1). If the utility commission would like to encourage buildings to switch to a TOU price structure to enforce change in electricity demand patterns, and at the same time wants to promote buildings to a higher RE investment, then some additional PBI makes it viable as described next. With PBI=1.5 ¢/kWh, the utility commission is flexible to set the off peak price of electricity anywhere from 42% to 100% of peak price. For all load profiles and PBI of 1.5 ¢/kWh, investment in renewable energy did not occur for any price ratio of 31% or less. The flexibility to set the TOU price is shown to be higher (see Figure 8) for PBI rate of 3.0 ¢/kWh. In this case, TOU of 10% or higher yields investment close to NZEB level.

Recall from Table 10, that we have examined a number of ratios from 0.02 to 1.0. For each ratio, we have selected a unique combination of off-peak and on-peak prices so that for all ratios the utility cost for base load is constant. Clearly, at higher ratios, the off-peak prices are higher, which encourage buildings to invest in RE. We have also seen earlier (in Figure 7) that a higher PBI promotes higher investment in RE. Hence, as seen in Figure 8, when the PBI is higher, even a smaller TOU ratio yields investment in RE. Thus, presence of a PBI gives more flexibility for the utilities to set TOU pricing while making it feasible for buildings (microgrids) to invest in RE based electricity generation.

Table 10: TOU pricing scheme scenarios for Tampa, Fl

scenario	Off Peak ($¢/kWh$)	On Peak ($¢/kWh$)	Ratio
1	0.698	30.900	0.02
2	1.698	28.408	0.06
3	2.698	25.915	0.10
4	3.698	23.422	0.16
5	4.698	20.930	0.22
Current	5.698	18.436	0.31
7	6.698	15.945	0.42
8	7.698	13.452	0.57
9	8.698	10.959	0.79
10	9.198	9.713	0.95
11	9.345	9.345	1.00

2.4.3.4 Joint Effect of Annual Rollover Compensation Rate and PBI

As per existing electricity regulation in Florida, the annual net metering rollover is compensated based on the annual avoided cost of a utility company. This rate is unknown for the coming years and depends on the variable costs of the company. In Figure 9, we have shown the RE investment levels at each load profile for different ratios of compensation

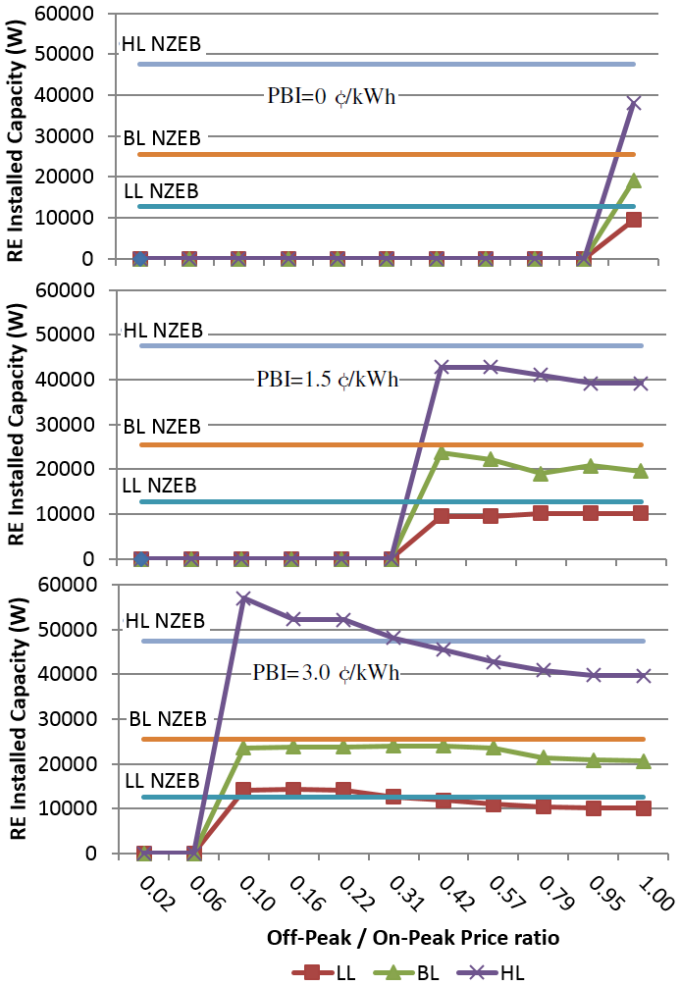

Figure 8: Sensitivity of TOU price of electricity for PBI= $0, 0.75, 1.50¢/kWh$

(0.1-1) and PBIs (0-2.5 ¢/kWh). The avoided cost paid by the utility company in Tampa in 2013 was about 30% of the standard rate for residential customers. We assumed a flat price of electricity of 9.345 (¢/kWh). Results presented in Figure 9 show that, for all load profiles and nonzero PBIs, for compensation ratios up to 0.7, the investment in RE is somewhat close to NZEB level and is not sensitive to the compensation ratio. Since the annual rollover compensation is rather low, the investment in solar energy generators did not rise higher than the customer's own energy needs, i.e., NZEB level. For some compensation ratios

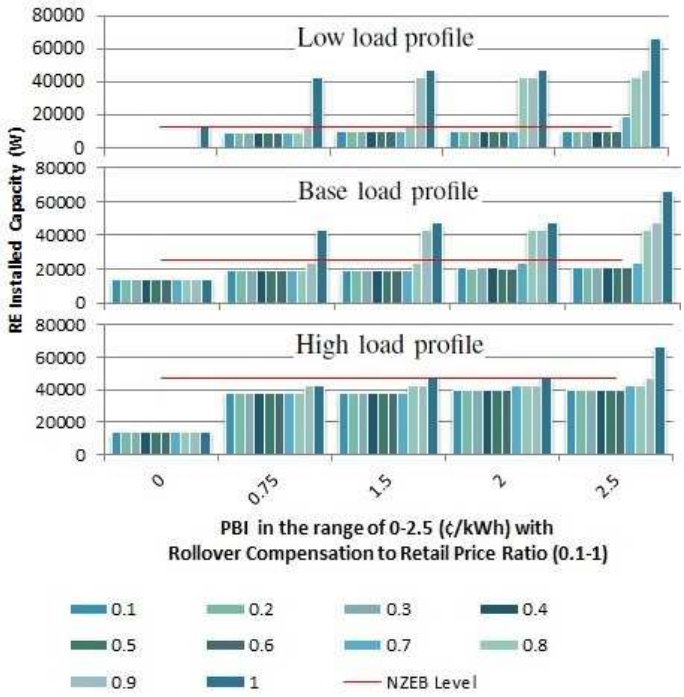

Figure 9: Design of the annual rollover compensation rate with different PBI levels - under flat price of electricity, for low, base, and high load profile buildings

(more than 0.7), the investment level increased beyond NZEB levels. At the higher levels of compensation, it is profitable for customers to invest in RE beyond their own needs and earn significant revenue at the end of the year. As shown in Figure 9, higher PBI makes it cost optimal to invest beyond NZEB level at relatively lower compensation ratios.

2.5 Conclusions

We have developed a mixed integer program model that yields optimal design of generating systems for buildings by considering the local weather data, load profile, available RE technology and cost, existing incentive programs, electricity tariffs, and minimum accepted ROI. The MIP model minimizes the total cost of investment and operation, and thus also yields optimal operational strategies for storage and trade with the grid.

The proposed model can be used by households, business sectors or investors to decide the most profitable portfolio of renewable generators and batteries to invest and operate. This decision support tool aims to optimally benefit from the available incentives and tax credits for green energy, and reducing the share of current power supply from fossil fuels thus reducing carbon dioxide emission and increasing social welfare in the long run. Also incentive and regulations sensitivity tool may be used by regulators to find the best combinations of incentives to maximize penetration of the distributed green power generation.

Numerical results show that incentive program parameters have threshold levels that promote different levels of investments in RE. The thresholds depend on the levelized cost of electricity (LCOE) for different RE sources, and, hence, are independent of the customer load profiles. Results show that as the incentives increase, the LCOE from RE decreases, eventually reaching below the average price of electricity from the grid. This makes it viable to invest in on-site electricity generation from RE sources to satisfy their own electricity needs. It is also shown that if the incentives continue to increase, buildings could invest in capacities beyond NZEB levels to earn a revenue.

Implementation of the model for buildings in different climates and load profiles demonstrates its utility as a tool to determine critical levels of incentives that are required to invest in a financially viable renewable energy system. In the next chapter, we have extended the work presented here to the development of a comprehensive model capable of optimizing over the joint parameter space of different incentive programs in a region. Our focus will be on design of financial incentive programs to promote net zero energy buildings. The model

can yield optimal incentive strategies comprising vectors of parameters. However, as the incentives considered here are offered by different government entities (federal, state, and local), a joint strategy would only be meaningful only if all entities can come together and implement it.

CHAPTER 3: DESIGN OF FINANCIAL INCENTIVE PROGRAMS TO PROMOTE NET ZERO ENERGY BUILDINGS[1]

3.1 Introduction

3.1.1 Background

Renewable energy (RE) driven electricity generation has become a fast-growing and opportunity-rich segment of energy industry over the past few years. The U.S. market, in particular, is experiencing an increasing growth in the number of new photovoltaic capacity installations. In 2014, there was around 6.2 GW of PV installation in the U.S., which is higher than 4.8 GW, 3.4 GW, and 1.9 GW in 2013, 2012, and 2011, respectively [4]. Wind energy industry has experienced a massive growth from 2005 to 2012 as well. New capacity installation has been 4.9 GW, 1.1 GW, 13.1 GW, and 6.7 GW in 2014, 2013, 2012, and 2011, respectively [5].

The aforementioned growth in electricity generation from RE installation can be attributed in part to both economic incentives offered by governments at all levels and also carbon emissions control strategies of the industrialized nations incorporating promotion of net zero energy buildings (NZEB) [3]. There are efforts both in the U.S. (Energy Independence and Security Act (EISA) of 2007 [35], [36]) and in Europe (the recast of the Directive on Energy Performance of Buildings, EPBD, adopted in May 2010 [37]) for implementing

[1]This chapter was partially published in [1]. Permission is included in Appendix C.

NZEB. The EISA 2007 sets the goal for NZEB to 50% of U.S. commercial buildings by 2040 and for all U.S. commercial buildings by 2050 [38]. In Europe, the EPBD established the target of reaching net zero status for all buildings that are either public owned or occupied by public authorities by 2018, and from 2020, all new buildings are to be net zero status [37].

In this paper, we present a mixed integer programming model and demonstrate its use for design of incentive programs (e.g., choice of production tax credit) that can make RE investments leading to NZEB status an economically viable option for commercial buildings. The MIP model obtains the RE investment strategy for given incentive levels while optimizing the total cost of meeting energy demand. The optimal cost strategy also results in an operational strategy for the building with regard to the RE generation, storage, and trade with the grid.

Despite the recent growth, there remain uncertainties in the investment in renewable energies. Risks and uncertainties for PV have been categorized into: 1) interannual solar variability, 2) photovoltaic technical performance uncertainty (PV degradation, inverter lifetime), and 3) market uncertainties. The two main sources of market uncertainty which can impact net revenues of PV are: 1) future electricity rate escalations and 2) future rate structures that could significantly modify the value of PV-generated electricity [9].

Investment in wind energy also must reckon with uncertainties from wind speed, equipment reliability, and market variabilities. Uncontrolled variability of electricity generation from wind and solar can be 10%/min and 10%/s, respectively [10]. Given the uncertainties

in renewable energy investment, any efforts to achieve NZE status for a building must carefully consider all incentives and regulations to ensure a discount rate based on an acceptable ROI. We consider six main categories of incentive programs available in the U.S. such as loan program, rebate, production tax credit (PTC), investment tax credit, renewable energy certificate (REC), and net metering. U.S. department of energy (DOE) provides loan guarantee for the purchase of renewable energy or energy efficient systems or equipment. Loan interest rate for commercial RE installations is based on the U.S. Treasury rate, the Federal Financing Bank (FFB) liquidity spread and project credit ratings[39]. Loan terms for commercial buildings are 90% of lifetime of the RE system. Rebate programs that are available in some regions are intended to reduce the initial investment costs.

PTC is a form of tax credit based on the amount of power generated by a RE system. The federal government in the U.S. is offering 30% tax credit for investment in RE and energy efficiency through Dec 31, 2016. Moreover, some states (e.g., New York) in the U.S. have their own state tax credit programs for RE investments. REC is a benefit to a building based on the amount of electricity it generates from RE, and customers may sell RECs back to the utility [12].

Finally, in our model we consider net metering as an incentive for buildings when there is flow of electricity both to and from the customer. We consider that the RE generation by buildings that exceeds its usage flows back to the grid. This offsets electricity consumed from the grid by the buildings. If there remains an annual rollover balance, the building is paid based on the avoided cost of the local utility company. In some regions, rollover is

calculated monthly and is paid at the full retail rate of electricity. Net metering is required by law in most states in the U.S. A complete list of incentive programs in the U.S. can be found in the database of state incentives for renewable energy and efficiency (DSIRE) [12].

Since the photovoltaic (PV) systems have high initial cost, they must be efficiently operated and maintained to deliver the expected benefits. This requirement serves as a barrier and pushes interested owners of residential and commercial buildings to participate in programs offered as third party ownership (TPO) solar finance companies. TPO allows the building owners to avoid the risk of investment while still reaping some of the rewards. TPO companies offer two main options: power purchase agreement (PPA) and solar lease [13]. In the PPA option, a customer is only charged upon electricity generation. In the lease option, a customer pays rent for the equipment irrespective of the amount of electricity generated.

We recognize the fact that NZEBs are also a class of microgrids. Henceforth, in this paper, we will use the terms NZEB and microgrid interchangeably. Some of the openly available optimization models design hybrid power systems (HPS) consisting of both renewable and non-renewable generators [18]. In general, a microgrid can be grid-connected [18], Stand-alone [16], or in a switchable mode between the two. A common operational strategy for microgrids considers optimal charging and discharging of energy storage devices, when available [14], [11], [23], [24].

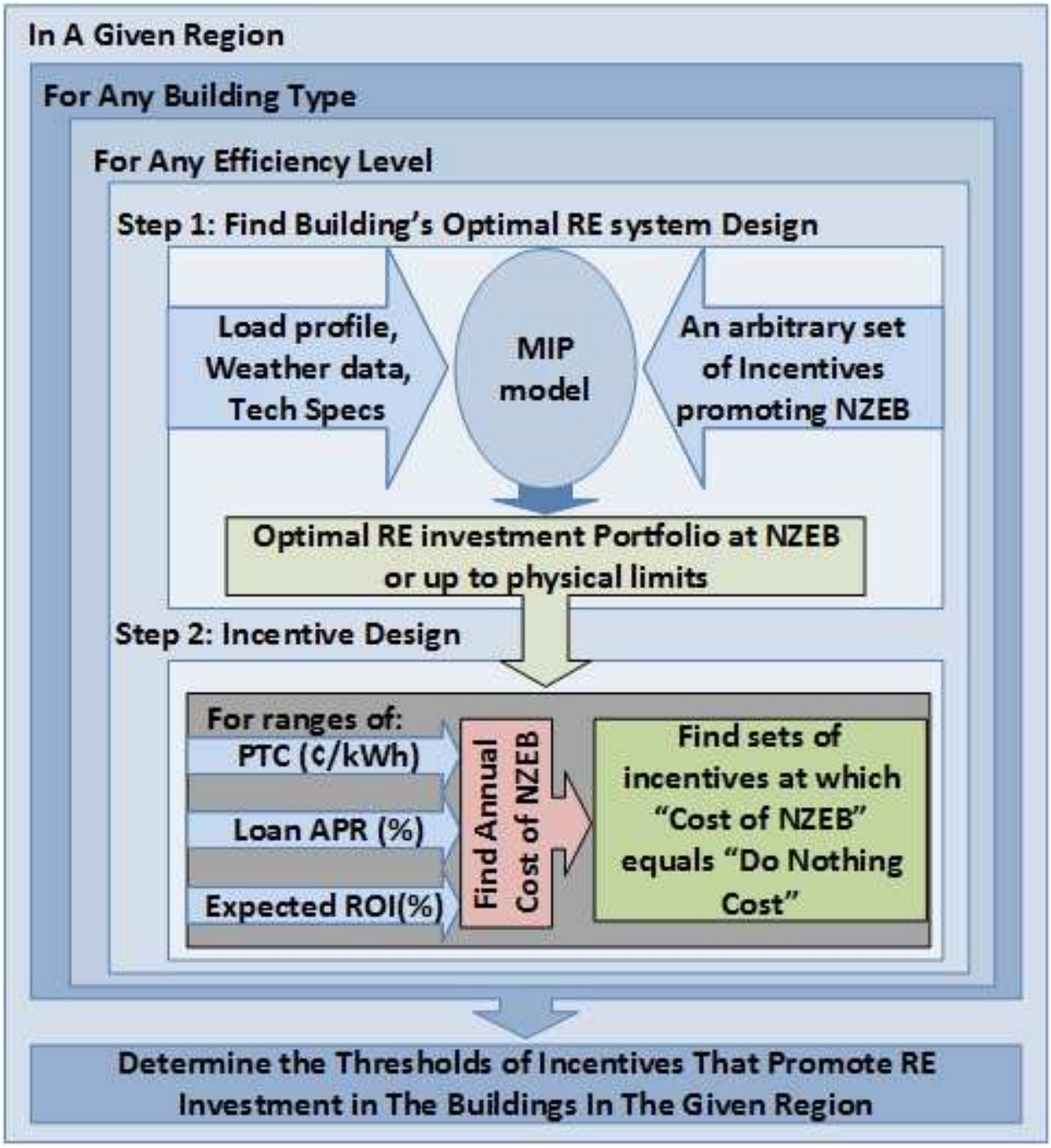

Figure 10: Modeling framework to design financial incentive programs

3.1.2 Contributions of This Chapter

Our MIP model is in essence similar to the distributed energy resources - customer adoption model (DER-CAM [40]). However, the key difference lies in how the model is purposed. Instead of the focus being on optimal design and operations (as in DER-CAM), our model is used to elicit incentives strategy design guidelines for policymakers promoting NZE status for commercial buildings. A broad range of incentives is considered explicitly in the model. The model use is demonstrated via exploration of answers to a number of key questions: What level of incentive might encourage a commercial building owner to invest in electricity generation from RE to seek NZE status? How do factors such as size and electricity load of a building, expected discount rates, and grid electricity price influence RE investment decisions in commercial buildings for a given incentive policy? Under current conditions, are commercial buildings likely to attain NZE status? Due to the page limitation of this exposition, we have presented samples of our analysis that generally addresses the above questions. Some of the key insights obtained from the model application are highlighted. One such insight is that given the current constraints of RE technology, installation area, and business, commercial buildings in general would need a significant load reduction through efficiency improvements in order to become NZEB through on-site RE generation. In fact, DOE recommends improving efficiency in the building as the first step towards being NZEB, before investing in RE technologies [41].

The schematic presented in Figure 10 shows the overall framework which consists of two main steps towards design of incentives, 1) the MIP model, 2) the economic model to

find optimal portfolio of incentives. First, the MIP is solved for the given type of building, assuming an arbitrary set of incentives at which the building type is encouraged to invest in RE up to the NZE level. This set of incentives can be found by trial and error with the MIP model. The MIP yields an optimal design of RE system. The RE system capacity may be lower than NZE if the installation area is limited. Knowing the optimal design of the RE system, we develop a cost equation using engineering economic principles. The cost equation incorporates the incentive parameters, loan interest rates, and the expected ROI. This equation is used to obtain the threshold of incentives and loan rate for a range of ROI. This threshold is a hyperplane. For each point on the hyperplane, the annual cost of the RE system is equal to the annual cost of buying electricity only from the grid as usual ("do nothing cost"). An example of such a threshold is depicted via a three dimensional plane in Figure 16.

For a given region, the following data is needed as input to the model: buildings' energy load profile for that climate, local weather data, current incentive programs, and electricity tariffs. We implemented the model for multiple building types, and different efficiency improvement levels. Experimental results are aimed at helping the policymakers to predict building owners' behaviors and find incentive levels that would stimulate more potential investors.

3.2 Model Formulation

3.2.1 Nomenclature

The notation used for the model is presented in Table 1 in chapter 2.

3.2.2 Other Model Preliminaries

In order to make the input data ready for the MIP model the following data pre-processing steps have been performed.

- PV module ($k = 1$) efficiency is calculated as a function of the operating temperature as follows [29]: $\eta^{k\ell t} = \eta^k_R - \zeta^k(T^{t\ell} - T_R)$.
- Solar radiation incident on a PV module surface, tilted by ρ° at latitude σ°, is calculated by $E^t = \frac{GHI^t \sin(\upsilon+\rho)}{\sin(\upsilon)}$, where $\upsilon = 90^\circ - \sigma + \delta$, and δ, the solar declination, equals $23.45^\circ + \sin(\frac{360}{365}(284 + day))$ [30].
- PV ($k = 1$) output power (DC) is calculated based on the hourly efficiency of solar installation ℓ as follows: $\omega^{k\ell t} = \eta^{k\ell t} E^t A^{k\ell} L^k_M L^k_R L^k_S L^k_D L^k_A L^k_C L^k_T,\ \forall \ell, t$
- Output power of the wind turbine has a non linear relation to the wind speed. As per [2], for each wind turbine ($k = 2$) with installation type ℓ, we have the following, where $a = \frac{\Gamma^{k\ell}_G}{\nu^3_r - \nu^3_{ci}}$ and $b = \frac{\nu^3_{ci}}{\nu^3_r - \nu^3_{ci}}$, $\forall i, t$:

$$\omega^{k\ell t} = \begin{cases} a(\nu^{t\ell})^3 - b\Gamma^{k\ell}_G & \nu_{ci} \le \nu^{t\ell} \le \nu_r, \\ \Gamma^{k\ell}_G & \nu_r \le \nu^{t\ell} \le \nu_{co}, \\ 0 & \text{o/w}, \end{cases}$$

In the model, we assume that NZEBs (microgrids) are grid-connected and operate under a net metering policy. The system components for a grid-connected NZEB are shown in Figure 11.

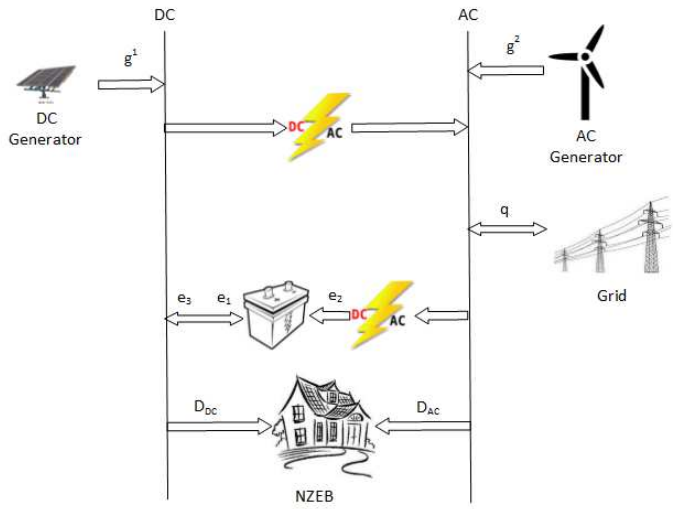

Figure 11: Elements of a grid-connected NZEB (microgrid) with PV and wind generation

3.2.3 MIP Model

Presented below is the complete MIP model that yields an optimal RE investment strategy for a building (microgrid) toward achieving a net zero energy status.

$$
\begin{aligned}
min\, Z = [\frac{n_u}{N}(\frac{\alpha u}{1-\frac{1}{(1+\alpha)^{n_u}}}) + \frac{\beta\frac{N}{n_B}(y_B F_B + x_B \Gamma_B V_B)}{1-\frac{1}{(1+\beta)^N}} \\
+\frac{\beta(\sum_k[\sum_\ell(y_G^{k\ell}F_G^{k\ell} + x_G^{k\ell}\Gamma_G^{k\ell}V_G^{k\ell}) - r^k] - u)}{1-\frac{1}{(1+\beta)^N}} \\
+\frac{\beta\sum_p \frac{N}{n_C^p} C_C^p x_C^p \Gamma_C^p}{1-\frac{1}{(1+\beta)^N}} + \psi\{(y_B F_B + x_B\Gamma_B V_B) + \sum_{k\ell}(y_G^{k\ell}F_G^{k\ell} + x_G^{k\ell}\Gamma_G^{k\ell}V_G^{k\ell}) + \sum_p C_C^p x_C^p \Gamma_C^p\} \\
-\sum_k a^k - \gamma_F \frac{1}{N}\frac{N}{n_B}(y_B F_B + x_B\Gamma_B V_B) - \gamma_F\frac{1}{N}\sum_k(\sum_\ell(y_G^{k\ell}F_G^{k\ell} + x_G^{k\ell}\Gamma_G^{k\ell}V_G^{k\ell}) - r^k) \\
-\gamma_F\frac{1}{N}\sum_p \frac{N}{n_C^p} C_C^p x_C^p \Gamma_C^p]/(1+\beta) + \frac{12\{D_1 h_1 + \frac{\sum_t D_2^t}{8760}h_2\}}{1+\frac{\beta}{2}} + \frac{h_0 + h + \lambda w}{1+\frac{\beta}{2}} \\
-\sum_t \frac{\sum_k I^k \sum_\ell g^{k\ell t}}{(1+\beta')^t} - \sum_t \frac{J\sum_{k\ell} g^{k\ell t}}{(1+\beta')^t}
\end{aligned}
\tag{3.1}
$$

$$S.t.\ g^{k\ell t} = \omega^{k\ell t} x_G^{k\ell} L_V^k\ \forall k, \ell, t \tag{3.2}$$

$$x_G^{k\ell} \leq y_G^{k\ell} G_{max} \forall k, \ell \tag{3.3}$$

$$x_B \leq y_B B_{max} \tag{3.4}$$

$$1 \leq 1 - \frac{\sum_t q^t}{\sum_t (\frac{(1-\Delta) D_{AC}^t}{L_{AC}} + \frac{(1-\Delta) D_{DC}^t}{L_{AC} L_{DC} \eta_2})} \leq 1 + \tau \tag{3.5}$$

$$\epsilon_1 (e_1^t + e_2^t) \leq x_B \Gamma_B \theta_1\ \forall t \tag{3.6}$$

$$e_1^t + e_2^t \leq \mu^t B_{max} \forall t \tag{3.7}$$

$$\epsilon_2^{-1} e_3^t \leq x_B \Gamma_B \theta_2 \forall t \tag{3.8}$$

$$e_3^t \leq (1 - \mu^t) B_{max} \forall t \tag{3.9}$$

$$\eta_1 [\sum_{k^1 \ell} g^{k^1 \ell t} + (e_3^t - e_1^t)] L_{DC} L_{AC} - \eta_1 (1 - \Delta) D_{DC}^t L_{DC}$$

$$+ \sum_{k^2 \ell} g^{k^2 \ell t} L_{AC} + q^t = (1 - \Delta) D_{AC}^t + \frac{1}{\eta_2} e_2^t \forall t \tag{3.10}$$

$$z^t = x_B \Gamma_B \forall l, t = 1 \tag{3.11}$$

$$z^t = (1 - \phi_1) z^{(t-1)} - \epsilon_2^{-1} e_3^t + \epsilon_1 (e_1^t + e_2^t) \forall t \geq 2 \tag{3.12}$$

$$z^t \geq \phi_2 x_B \Gamma_B \forall t \tag{3.13}$$

$$z^t \leq x_B \Gamma_B \forall t \tag{3.14}$$

$$\sum_{k\ell} g^{k\ell t} + (e_3^t - e_1^t) - (1 - \Delta) D_{DC}^t \leq x_C^p \Gamma_C^p \forall t, p = 1, k \in k^1 \tag{3.15}$$

$$\frac{1}{\eta_2} e_2^t \leq x_C^p \Gamma_C^p\ \forall t, p = 2 \tag{3.16}$$

$$D_2^t \geq q^t\ \forall t \tag{3.17}$$

$$D_1 \geq D_2^t\ \forall t \tag{3.18}$$

$$h \geq \sum_t q^t H^t \tag{3.19}$$

$$w = \sum_t q^t H^t - h \tag{3.20}$$

$$\sum_{k\ell} \sum_{t'=t}^{t+M} g^{k\ell t'} + z^t \geq \sum_{t'=t}^{t+M} (1-\Delta)(D_{AC}^{t'} + D_{DC}^{t'}) \forall t \tag{3.21}$$

$$A^{k\ell} x_G^{k\ell} \leq \overline{A}^{k\ell} \ \forall \ell, k = 1 \tag{3.22}$$

$$A^{k\ell} y_G^{k\ell} \leq \overline{A}^{k\ell} \forall \ell, k = 2 \tag{3.23}$$

$$\sum_\ell y_G^{k\ell} \leq 1 \ k = 2 \tag{3.24}$$

$$r^k \leq R^k \sum_\ell x_G^{k\ell} \Gamma_G^{k\ell} k = 1 \tag{3.25}$$

$$r^k \leq R^k \sum_{\ell t} g^{k\ell t} k = 2 \tag{3.26}$$

$$r^k \leq \overline{R}^k \ \forall k \tag{3.27}$$

$$u \leq \overline{U}_2 [\sum_p x_c^p C_C^p \Gamma_C^p + x_B V_B \Gamma_B + y_B F_B + \sum_k (\sum_\ell [y_G^{k\ell} F_G^{k\ell} + x_G^{k\ell} \Gamma_G^{k\ell} V_G^{k\ell}] - r^k)] \ \forall k \tag{3.28}$$

$$u \leq \overline{U}_1^k \ \forall k \tag{3.29}$$

$$a^k \leq \gamma_s^k \sum_\ell (y_G^{k\ell} F_G^{k\ell} + x_G^{k\ell} \Gamma_G^{k\ell} V_G^{k\ell}) \ \forall k \tag{3.30}$$

$$a^k \leq \overline{a}^k \ \forall k \tag{3.31}$$

$$x_G^{k\ell}, x_C^p, x_B \in \mathbb{Z}^+ \cup \{0\}, \ q^t, w \in \mathbb{R}, \ y_G^{k\ell}, y_B, \mu^t \in \mathbb{B} \ g^{k\ell t}, u, r^k, z^t, e^t, D_1, D_2^t h, a^k \in \mathbb{R}^+ \cup \{0\} \tag{3.32}$$

The investment and financing time horizon considered in the model are 30 years. All capital costs and credits are depreciated over 30 years in addition to other annual costs and

revenues. We annualized all costs and revenues in the MIP model in the objective function, aiming at minimization of the overall cost of electricity in a building for a typical year. The positive elements of the objective function (A.1) represent equivalent annual cost and the negative elements indicate yearly revenue or credits. The seven cost elements indicate, in order presented in (A.1), the loan annual payment, depreciated annual cost of capital used for technology procurement and installation (including fixed and variable costs of batteries, generators, and converters), annual operation and maintenance costs, and billing demand and peak billing demand charges. The last positive element of the objective function represents the basic service charge of the utility company in addition to the cost of net electricity purchase from utility (when $h \geq 0$) or revenue from annual rollover compensation (when $\omega < 0$). The revenue/credits comprise rebates, state tax credit, federal tax credit for capital investment (in batteries, generators, and converters), the production tax credit (PTC),and renewable energy certificate (REC).

The constraints are as follows. Constraint (3.2) calculates electricity generation by each type of generator based on the corresponding weather data and the derate factor of availability. Constraints (3.3,3.4) are to include fixed cost associated with the installation of the system, i.e., if $x_G^{k\ell}$ takes a positive value, the inequality forces $y_G^{k\ell}$ to take one as well, and similar for y_B. Constraint (3.5) is the NZEB constraint, which one may include in the model only if imposing NZE status. It forces the building to invest in RE generators at NZE level regardless of the extra costs. It is useful to find the extra cost of achieving NZE status comparing to do nothing cost. The constraint forces the ratio of demand satisfied by on-site

RE to one. Setting the constraint as an inequality helps to avoid infeasibility of forcing the RE level to be exactly equal to one. Giving the constraint a tolerance of τ lets the building go beyond the NZEB a little if needed in optimal case. Constraints (3.6) and (3.7) show the rate of charge of the batteries considering charging efficiency and nominal charging rate. Constraints (3.8) and (3.9) show the rate of discharge of the batteries considering discharging efficiency and nominal discharging rate. In (3.7) and (3.9), μ^t ensures that a battery is not charged and discharged at the same time t. Balance constraint (3.10) ensures that the energy input to a microgrid equals its output, both for DC and AC, at all times. Constraints (3.11) through (3.14) accomplish hourly updates of the battery capacities. Power conversion from DC to AC and vice versa is always limited by the capacities of inverters (3.15) and rectifiers (3.16).

It is considered that the utility gives credit to the microgrids for selling electricity back to the grid. As practiced by many states in the U.S., if total yearly sales credit exceeds total purchase of a building, the utility pays for the excess credits to the consumer. The constraints (3.17) and (3.18) calculates annual peak and base demand of the building for electricity from the grid. The constraints (3.19) and (3.20) calculate annual electricity payment to the utility company, if any, and sales credits, respectively. To ensure that the customer has power during blackouts for at least M hours (reliability), we added constraint (3.21) to the model. The installation capacity limits for generating devices are handled by (3.22) through (3.24). Constraints (3.25) through (3.31) accounts for the rebate, loan, and state tax credit amounts resulting from the investment plan.

3.2.4 Key Outputs from the MIP

- Annual extra cost of NZEB ($C_{NZEB}, \%$)

$$C_{NZEB} = 100(\frac{Z^\star}{Z_0} - 1), \text{ Where } Z_0 \text{ is "Do Nothing" cost.}$$

- Percentage of demand satisfied by on-site RE ($RE, \%$)

$$RE = 100(1 - \frac{\sum_t q^t}{\sum_t (D^t_{AC}(1-\Delta)/L_{AC} + D^t_{DC}(1-\Delta)/(L_{AC}L_{DC}\eta_2))})$$

- Overnight cost of installed RE system ($C_{RE}, \$/W$)

$$C^k_{RE} = \frac{F^k_G y^k_G + \sum_\ell V^k_G x^{k\ell}_G \Gamma^{k\ell}_G - r^k}{\sum_\ell x^{k\ell}_G \Gamma^k} + \frac{C^p_C x^p_C \Gamma^p_C}{\sum_{k\ell} x^{k\ell}_G \Gamma^k_G}$$

- Overnight cost of installed energy storages ($C_B, ¢/Wh$)

$$C_B = \frac{y_B F_B + V_B x_B \Gamma_B}{x_B \Gamma_B}$$

3.2.5 Incentive Program Design

The required input parameters for the incentive design formulation are optimal NZEB design ($x^{\star k\ell}_G$ and $x^{\star p}_C$). In case of considering energy storages in the NZEB, $x^\star_B$ and $q^{\star t}$ (optimal operation of NZEB) are needed as well.

Given the optimal design (and operation), i.e., assuming $x^{k\ell}_G = x^{\star k\ell}_G$, $x^p_C = x^{\star p}_C$, $x_B = x^\star_B$, (and $q^t = q^{\star t}$), the followings can be calculated:

$g^{k\ell t}$ from (3.2), $y^{\star k\ell}_G$ and $y^\star_B$ from (3.3) and (3.4) respectively, D^t_2 (billing demand) and D_1 (peak billing demand) from (3.17) and (3.18) respectively, h and w (netmetering bill or credit) using (3.19) and (3.20) respectively, r^k (rebates) via (3.25) through (3.27), u (loan amount) using(3.28) and (3.29), and a^k (state tax credit) via (3.30) and (3.31).

Considering PTC is the same for different energy sources, we have $PTC = I^k, \forall k$. Having calculated all the above mentioned variables, the annual cost of the NZEB in (A.1) is now only a function of the following parameters: loan interest rate (α), discount rate (β), and production tax credit (PTC). We define such a function as $\Lambda(\alpha, \beta, PTC)$, which can be used to obtain the annual cost of NZEB for given set of α, β and PTC values.

Calculating "Do Nothing" cost can be done with a similar approach. Setting $x_G^{k\ell} = 0$, $x_C^p = 0$, $x_B = 0$ makes the defined Λ function, only dependent to β, i.e., the net present value of the annual electricity bill is only a function of discount rate. So let $\Lambda^\circ(\beta)$ be the do nothing cost for the building.

Then the threshold for the portfolios of incentives at which the NZE status becomes a financially viable option for the building, could be found by solving the following equation:

$$\Lambda(\alpha, \beta, PTC) = \Lambda^\circ(\beta)$$

Any combination of α, β, and PTC that satisfies the equation would be a solution. The set of solutions forms a three dimensional hyperplane which represents the optimal threshold for the incentive parameters. The example of such a hyperplane can be seen in Figure 16). In this paper we investigated PTC selection for the Tampa area (in the state of Florida) for buildings with different financial status.

However the model can be generalized for a higher number of incentives including investigate rebates ($R^k, \overline{R}$), state tax credit($\gamma_s^k, \overline{a}^k$), federal tax credit ($\gamma_F$), and PTC ($I^k$) all together and find optimal threshold for the combinations of these incentive programs for

buildings in a region. In that case, an eight dimensional hyperplane for the threshold of incentives can be found using the following equation:

$$\Lambda(\alpha, \beta, PTC, R^k, \overline{R}, \gamma_s^k, \overline{a}^k, \gamma_F) = \Lambda^\circ(\beta)$$

Note that solving the MIP model is a necessary step as it estimates an optimal NZE portfolio of technology ($x_G^{\star k\ell}$, $x_C^{\star p}$, $x_B^\star$, and $q^{\star t}$) that a building type in a region would choose to invest in, if it is financially viable. In case of not having enough area to be optimally NZEB via on-site RE generation, the size of the portfolio would be up to the physical limits of the building.

3.3 Model Implementation

We have examined the impact of financial incentive programs using the MIP model in the context of transforming three categories of commercial buildings in Tampa-Florida into NZEBs. We first provide the description and values of the different categories of input parameters to facilitate understanding the results. We then present the results in two parts: 1) the optimal investment level in RE generation of a building under an arbitrary set of incentives at which the building will be encouraged to invest in RE, and 2) use the results from the MIP model to determine the critical threshold values of financial incentive programs that promote NZE status. We used CPLEX to solve the MIP model on a standard desktop computer with 16 GB RAM and Intel i7 processor @2.93 GHz. The station took on average 30 seconds to solve the MIP model for different building types and incentive combinations. The solution gap was set to 0.2%.

3.3.1 Data

3.3.1.1 Building Data

The characteristic features of the buildings that are used as input for the MIP model are the available area for on-site installation, and hourly electricity load data. The buildings used in the computational study are from the U.S. Department of Energy (DOE) commercial reference buildings [42]. The electricity load data were obtained from building energy analysis data developed using EnergyPlus simulation software [32]. DOE developed 16 commercial reference building types and three construction categories, in 16 climate zones, which represent approximately 70% of the commercial buildings in the U.S.

In Figure 12, we present an overview of the 16 building types in Tampa in terms of their annual electricity load (with and without 40% load reduction via increased efficiency) and their estimated potential on-site solar energy generation. Potential annual on-site solar energy generation in Tampa buildings is calculated based on the following assumptions: 1) capacity factor of 20%, 2) ground coverage ratio of 0.8, and 3) power density value of $193\frac{W}{m^2}$. Figure 12 illustrates that the available area for RE installation could pose a barrier for some of these buildings to become NZEB using on-site RE generation.

Clearly there are three groups of commercial buildings in the figure:1) buildings with abundant roof area for solar installation, thus no physical constraint to be NZEB, 2) buildings with limited roof area that are required to reduce their load through efficiency improvements in order to attain NZE status with on-site RE generation, and 3) buildings that even with 40% reduction in load cannot be NZEB due to their very limited roof area for solar installation

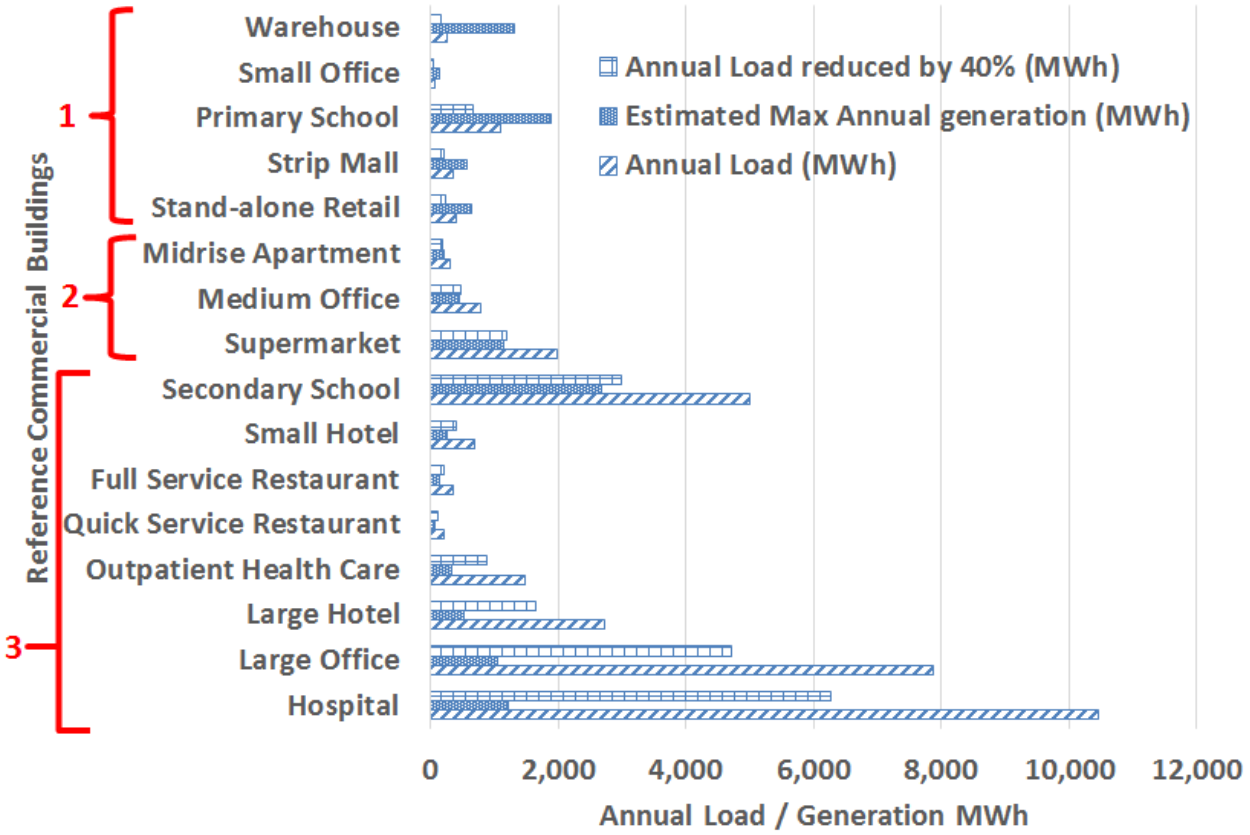

Figure 12: Potential to be NZEB using on-site solar energy generation in Tampa, Fl

in comparison with their load. The buildings in group 3 may attain NZE status using off-site RE generation. Since a significant portion of off-site RE generation cost is the price of land which varies significantly even within a certain region, we did not consider off-site RE generation in designing financial incentive programs to promote NZEB.

3.3.1.2 Incentives/Regulations

In Tables 11 and 12, we have listed all of the currently available incentives and regulations for commercial RE installations in Tampa, FL.

Table 11: RE incentive programs for commercial buildings in Tampa, FL

Item	Amount
Business Energy Investment Tax Credit	30% of total investment
RE Production Tax Credit	1 ¢/kWh up to $1M
DOE Loan Program	Loan term = Min{30 years, 90% projected life of financed assets}
Sales Tax Incentive	All sales tax on solar energy system, no limit
Regulatory Policy	REC and Net-Metering at avoided cost rate (3.067 ¢/kWh in 2014 [43])

Table 12: Time-of-day general service demand (GSDT) in Tampa, FL

Item	Amount
Basic service charge	30 ($/month)
Demand charge	4.63 ($/kW) of billing demand & 6.10 ($/kW) of peak billing demand
Time of Day price	On-peak: 7.417 (¢/kWh) & Off-peak: 5.223 (¢/kWh)
Peak hours	Nov-Mar (Winter) : 6:00AM-10:00AM & 6:00PM-10:00PM Apr-Oct (Summer) : Noon-9:00PM

3.3.1.3 Technology Options

The technology options considered in our model are PV panels, wind turbines, batteries, inverters, and rectifiers. Tables 13 and 14 provide specifications of these options and their corresponding costs, respectively [44].

We have assumed the PV panels are installed at a tilt angle 26.5° based on the latitude of the location (28°). The cost of each model includes the costs of mount and wirings. For both wind and solar generators and inverter, the MIP model finds the optimal capacity to invest with increment of 100 W. For investment in the battery (energy storage), capacity increment of 100 Wh is considered.

Table 13: RE generation technology specifications

	Technology				
Specifications	PV	Wind	Battery	Inverter	Rectifier
Life (yrs)	30	30	5	10	10
Size (W)	100	100	100	100	100
Implementing area (m^2)	0.516				
efficiency (%)	20				
Wind Tower base area (m^2)		18			
Cut in (m/s)		3			
Rated power speed (m/s)		12.5			
Cut out (m/s)		25			
$\theta_1(\%)$			30		
$\theta_2(\%)$			50		
$\epsilon_1(\%)$			90		
$\epsilon_2(\%)$			90		
CEC Efficiency				96	99.9

Table 14: Non-residential turnkey system installed costs

Technology	Fixed Cost ($) (based on 200kW system)	Variable Cost ($/W , $/Wh)
Solar	65k	1.72
Wind	20k	2.00
Battery	5k	0.25
Inverter	included in solar fixed costs	0.15
Rectifier	included in battery fixed cost	0.02

Per information made available in [44], solar installation costs are based on a 200-kW DC rooftop system with standard crystalline silicon modules and flat roof with minimal obstructions. We assume the cost components of design, engineering, permitting, and direct labor to be part of the fixed cost, which remain constant for systems of size 150kW to 250kW. The variable costs for each technology consist of electrical balance of system (BOS), structural BOS, supply chain, overhead, and margin, in addition to the cost of the equipment. Figure 13 demonstrates the relationship between total cost and the size of they system.

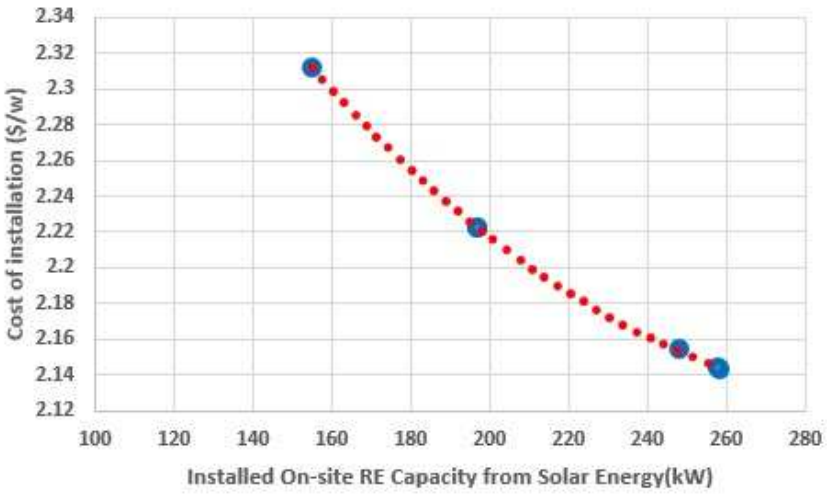

Figure 13: RE installation cost vs. capacity

Particularly, due to the impact of fixed cost, as the size of the system increases, the total cost will decrease. Besides these costs, an O&M cost with a coefficient of 2% is considered in the model.

3.3.1.4 Local Weather Data

The hourly historical data on solar radiation, wind speed level, and ambient temperature for Tampa-FL are considered based on typical meteorological year 3 from NREL [45].

3.3.2 Computational Study

In the rest of this paper we demonstrate how the results of the MIP model can be used to design incentive programs that promote RE investment and likely NZE status for commercial buildings. The annual on-site electricity generation of NZEBs satisfies the load and the losses in the system under a net-metering policy. To examine the impact of incentive program design on different types of commercial buildings, we chose to analyze buildings from each of the three groups mentioned in Figure 12. We selected Stand-alone retail, medium

office, and outpatient health care building from groups 1, 2, and 3, respectively. Among the financial incentive programs available in Tampa for commercial buildings (listed in Table 11 and 12), we used the given values for the sales tax incentive, business energy investment 30% tax credit (ITC), REC, and net-metering in all scenarios. The experiments were conducted for all three buildings, assuming investors' acceptable cash flow discount rates in the range of 0.001 - 10%, and with and without load reduction through efficiency improvement.

3.3.2.1 Model Calibration

We calibrated the MIP model using the data based on the "Do Nothing" case. Setting $x_G^{k\ell} = 0$, $x_C^p = 0$, and $x_B = 0$. That is, we computed the cost of the "Do Nothing" case, where the hourly purchase of electricity from the grid should match the load profile of the building. The "Do Nothing" cost is equal to the total electricity bill paid to the utility company.

3.3.2.2 Energy Storage in Tampa, Fl

The results showed that investing in energy storages is not an optimal decision, which can be explained as an effect of the existing net-metering policy. However, if the profit from storing power during off-peak hours is assumed to be higher, then investment in battery storage becomes financially viable.

3.3.2.3 MIP Solution for Different Input Incentives

As depicted in Figure 10, in step 1 we obtain the optimal RE system design, $(x_G^{k\ell}, x_C^p)$ for which we need as input a set of incentives that promotes RE investment. In order to obtain such a set of incentives, we solved the MIP for numerous combinations of loan rate and PTC (see Figure 14). We observed three zones of incentive combinations: do nothing

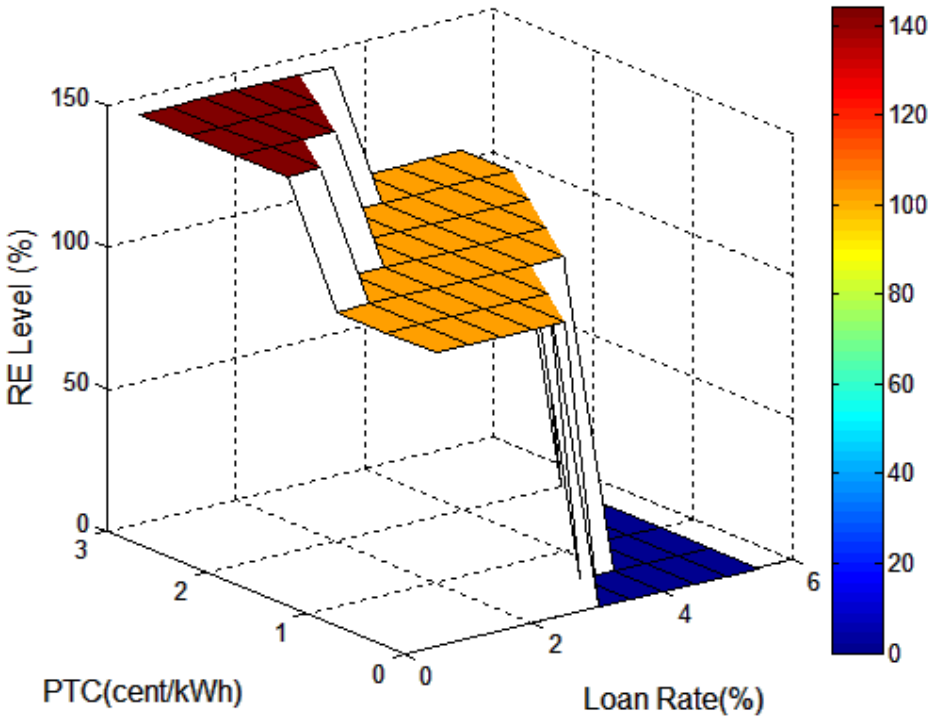

Figure 14: Stand-alone retail building's RE investment level (as % of load)

(0% RE), invest at NZEB (100% RE), and invest beyond NZEB (> 100% RE). Any of the incentive combinations corresponding to 100% RE could be used in step 1. Note that for buildings with insufficient area, maximum RE level achievable would be below NZE level (< 100% RE). In such cases, any incentive combinations promoting RE investment could be used as input to step 1. However finding a suitable set of incentive combination for step 1 can be done via trial and error. Different incentive combinations can be evaluated until we obtain one that promotes the NZEB investment or one that promotes RE below NZEB level and up to the installation area limit.

3.3.2.4 Investment vs. "Do Nothing" Case

Figures 15 illustrates the cost burden resulted by forcing NZE status, based on a 2% discount rate on the cash flow.

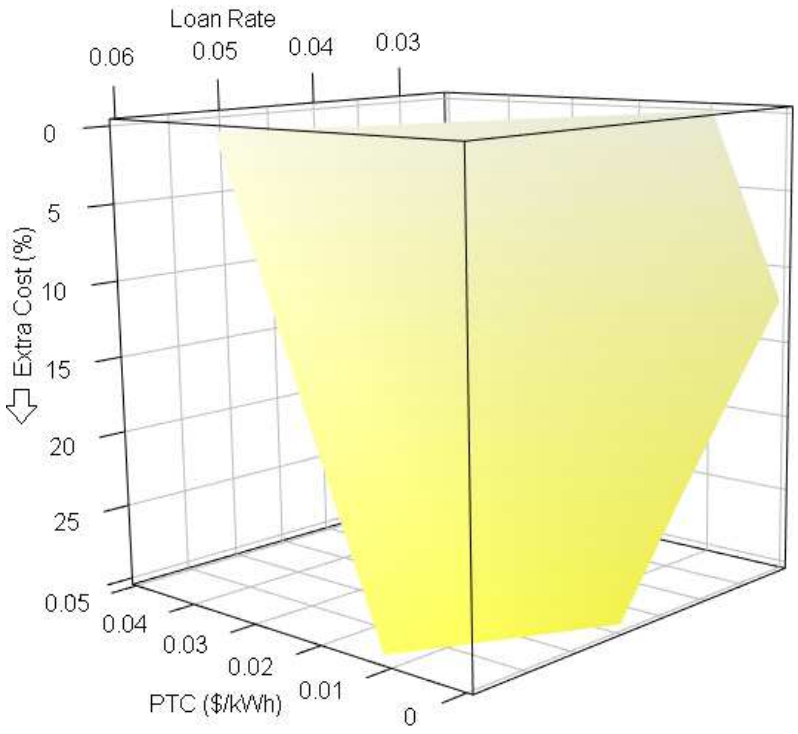

Figure 15: Stand-alone retail building's extra cost due to forced NZE status compared to "Do Nothing" case

The figure can be interpreted as follows. Consider a Stand-alone retail building with discount rate of 2%, project credit rating of A+ (eligible for a loan of an interest about 3.33%), and at current PTC in Tampa, FL of 1 ¢/kWh. Per Figure 15, this building will have about 6.3% increase in its annual cost of energy comparing to "Do Nothing" cost. This extra cost should be compensated through other incentive forms if NZE status is sought.

3.3.2.5 Optimal Threshold of Incentive Portfolios

Stand-alone retail building has an annual energy load of 412.1 MWh and has enough rooftop area to install solar panels to satisfy all its own needs. As can be seen in Figures 14-18, the viability of investment depends on both incentives, especially the loan interest rate (project credit rating). Since the threshold for the incentive parameters are not easily deci-

pherable from the three-dimensional plots (Figures 16), we have provided the two dimensional threshold curves, for all building types, for investors' discount rate of $\beta = 2\%$ in Figure 17. Similar two dimensional images of the higher dimensional policy threshold hyperplane can be produced using other discount rate values. Figure 17 demonstrates the financial viability threshold for NZEB status for different loan rate and PTC combination at 2% discount rate for different types of commercial buildings. As can be seen, different buildings respond similarly to the incentive programs. This observation makes it easier for the policymaker to design a set of incentive programs that can appeal to a greater audience.

In Figure 18, plot A shows for a Stand-alone retail building in Tampa, how a 30% reduction in load changes the optimal threshold of the incentive program in the same building comparing to the base load. A reduction in load changes the threshold in two ways: 1)lower load results in a lower "do nothing cost", 2)a lower load requires lower RE capacity to achieve the NZEB level, which imposes a higher \$/W cost of investment (see Figure 13). Both of the above reasons make the investment less attractive for the building compared to the "Do Nothing" case. Hence a higher level of incentive is required to make NZEBs financially viable after efficiency improvement.

Figure 18 plot B shows the optimal threshold of PTC and loan rates for Stand-alone retail building for two levels of discount rates, 2% and 7%. This illustrates an increment in PTC can significantly increase the ROI of the RE project for the building.

Medium office building has an annual energy load of 786.4 MWh and insufficient roof area to install solar panels to be NZEB. However, with about 46% load reduction through

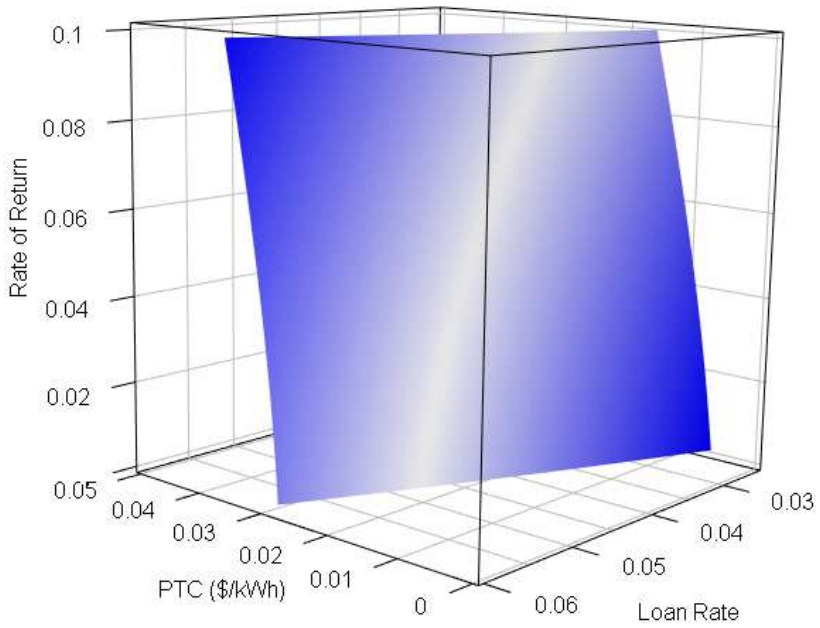

Figure 16: NZE attainable combinations of loan rate, PTC, and return on investment (stand-alone retail without efficiency improvement)

efficiency improvement and load management, it would be capable of reaching NZE status through on-site RE generation. The efficiency improvement does not have a significant impact on its investment size and just slightly decrease it from 257.4 kW to 248 K. Outpatient health care unit building has an annual energy load of 1495.3 MWh. Due to its high load relative to the roof area, it cannot turn to NZEB through on-site RE generation even with 50% reduction in load and invest in a 196.5 kW system in both cases. In medium office and outpatient health care unit buildings in Tampa, FL, we observed an impact of the load reduction and discount rates on optimal thresholds of incentives, similar to the one discussed for the stand alone building.

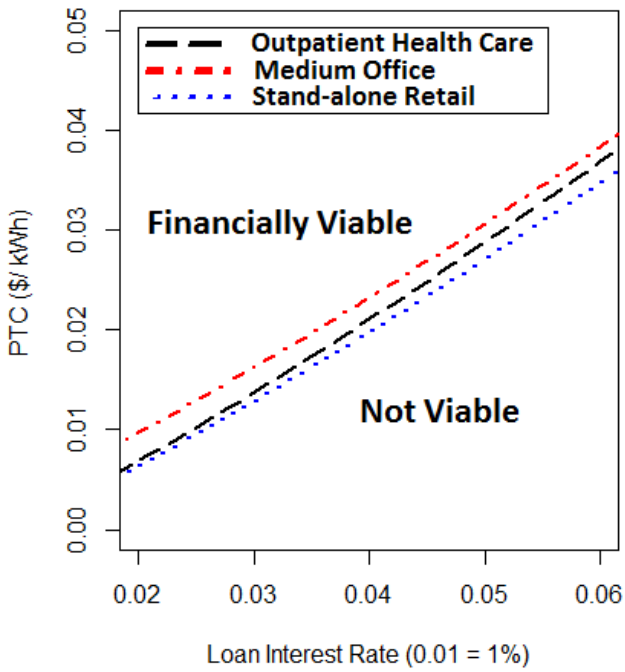

Figure 17: NZE attainable combinations of loan rate and PTC, at 2% return on investment for three commercial buildings from three categories (buildings without efficiency improvement)

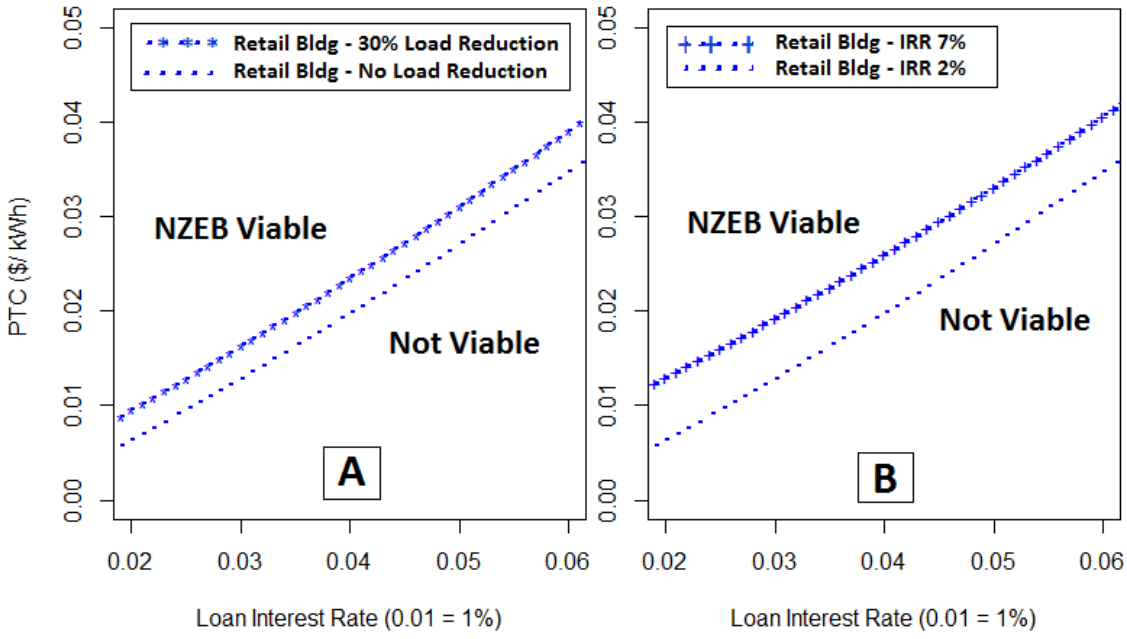

Figure 18: NZE attainable combinations of loan rate and PTC, for Stand-alone retail buildings in Tampa, FL: Graph A- with and without 30% load reduction (with ROI=2%), Graph B- with expected ROI of 2% and 7% and no load reduction

Table 15: Who will invest with PTC = 1.5 ¢/kWh in Tampa, FL?

Discount Rate: DR; Buildings; R: Retailer; O: Office; H: Health Unit										
		DR = 2%			DR = 4%			DR = 6%		
Project Credit Rating	APR (%)	R	O	H	R	O	H	R	O	H
AAA	3.25	+	-	+	-	-	-	-	-	-
AAA-	3.25	+	-	+	-	-	-	-	-	-
AA+	3.25	+	-	+	-	-	-	-	-	-
AA	3.25	+	-	+	-	-	-	-	-	-
AA-	3.29	+	-	+	-	-	-	-	-	-
A+	3.33	+	-	+	-	-	-	-	-	-
A	3.37	-	-	+	-	-	-	-	-	-
A-	3.44	-	-	-	-	-	-	-	-	-
BBB+	3.52	-	-	-	-	-	-	-	-	-
BBB	3.59	-	-	-	-	-	-	-	-	-
BBB-	3.78	-	-	-	-	-	-	-	-	-
BB+	3.98	-	-	-	-	-	-	-	-	-
BB	4.18	-	-	-	-	-	-	-	-	-
BB-	4.38	-	-	-	-	-	-	-	-	-
B+	4.55	-	-	-	-	-	-	-	-	-
B	4.73	-	-	-	-	-	-	-	-	-
B-	4.88	-	-	-	-	-	-	-	-	-

3.3.2.6 Now Who Will Really Invest in RE?

The financial status of a commercial building is the key to answer this question. We determined the financial classes for commercial buildings via two measure, credit rating and expected ROI (discount rate on cash flow). We have shown through our analysis the optimal threshold for the incentive portfolios to encourage NZEB. Now, policymaker can evaluate the impact of a choice of portfolio of incentives on several classes of commercial building in the given region, such as Tampa.

Results show, at current level of PTC incentive in tampa, 1¢/kWh, investment in RE is not cost effective for the three building types we have examined for discount rates of 2, 4,

Table 16: Who will invest with PTC = 2.0 ¢/kWh in Tampa, FL?

Discount Rate: DR; Buildings; R: Retailer; O: Office; H: Health Unit										
		DR = 2%			DR = 4%			DR = 6%		
Project Credit Rating	APR (%)	R	O	H	R	O	H	R	O	H
AAA	3.25	+	+	+	+	-	+	-	-	-
AAA-	3.25	+	+	+	+	-	+	-	-	-
AA+	3.25	+	+	+	+	-	+	-	-	-
AA	3.25	+	+	+	+	-	+	-	-	-
AA-	3.29	+	+	+	+	-	+	-	-	-
A+	3.33	+	+	+	+	-	+	-	-	-
A	3.37	+	+	+	+	-	+	-	-	-
A-	3.44	+	+	+	+	-	+	-	-	-
BBB+	3.52	+	+	+	+	-	+	-	-	-
BBB	3.59	+	+	+	+	-	+	-	-	-
BBB-	3.78	+	-	+	-	-	-	-	-	-
BB+	3.98	+	-	+	-	-	-	-	-	-
BB	4.18	-	-	-	-	-	-	-	-	-
BB-	4.38	-	-	-	-	-	-	-	-	-
B+	4.55	-	-	-	-	-	-	-	-	-
B	4.73	-	-	-	-	-	-	-	-	-
B-	4.88	-	-	-	-	-	-	-	-	-

and 6%. These results are based on the aforementioned assumptions on costs of technologies and installation, electricity tariff, and typical weather data, etc.

The same evaluation has been done for higher PTCs of 1.5, 2, and 2.5 ¢/kWh. Tables 15, 16, and 17 demonstrate the response of different classes of commercial buildings to a given incentive level, where if a class of building invest in RE shown as (+) and otherwise as (-).

Using this evaluation tool, the impact of incentive programs is now more clear to the authorities. Ideally, with actual number of buildings in each class in Tampa area, the policymaker can even have a richer tool to evaluate the impact. The Tables illustrate that an increase in PTC level can significantly increase the number of classes of commercial

Table 17: Who will invest with PTC = 2.5 ¢/kWh in Tampa, FL?

Discount Rate: DR; Buildings; R: Retailer; O: Office; H: Health Unit										
		DR = 2%			DR = 4%			DR = 6%		
Project Credit Rating	APR (%)	R	O	H	R	O	H	R	O	H
AAA	3.25	+	+	+	+	+	+	+	+	+
AAA-	3.25	+	+	+	+	+	+	+	+	+
AA+	3.25	+	+	+	+	+	+	+	+	+
AA	3.25	+	+	+	+	+	+	+	+	+
AA-	3.29	+	+	+	+	+	+	+	+	+
A+	3.33	+	+	+	+	+	+	+	+	+
A	3.37	+	+	+	+	+	+	+	+	+
A-	3.44	+	+	+	+	+	+	+	+	+
BBB+	3.52	+	+	+	+	+	+	+	-	+
BBB	3.59	+	+	+	+	+	+	+	-	+
BBB-	3.78	+	+	+	+	+	+	+	-	+
BB+	3.98	+	+	+	+	-	+	-	-	-
BB	4.18	+	+	+	+	-	+	-	-	-
BB-	4.38	+	-	+	-	-	-	-	-	-
B+	4.55	+	-	+	-	-	-	-	-	-
B	4.73	+	-	+	-	-	-	-	-	-
B-	4.88	-	-	-	-	-	-	-	-	-

buildings who can invest in RE at NZEB level or up to their limits (below or above NZEB). Given the results from our analysis, one can come up with different policy-design approaches. For example, for a RE loan application from a commercial building, the bank can evaluate financial viability of the RE installation in that building and guide the applicant.

The bank determines the proper loan interest rate based on the applicant's risk and other market considerations as follows: Interest Rate = Applicable U.S. Treasury Rate for the tenor of the loan + 37.5 basis points (0.375%, the Federal Financing Bank (FFB) liquidity spread) + Credit-Based Interest Rate Spread (A range of 0.0% to 1.625% for project credit ratings of range AAA to B-, see Table17 for credit ratings and estimated interest rates). U.S. treasury rate varies daily, the mean and median of the 30 years rate is 2.83% and 2.89%

respectively. In this study we considered 2.89% as U.S. treasury rate for the tenor of the loan. Also a 20% down payment for loans is assumed. Ultimately, given the interest rate, the authority may investigate the financial viability of a RE project using optimal thresholds.

In addition, our model can provide investment consultation services to commercial buildings that are interested in satisfying a portion, if not all of, their demand through renewable energies. Knowing their credit rating, expected ROI and local incentives for RE such as PTC, we can help the buildings decide for their energy supply methods.

3.4 Conclusions

This paper presents an economic framework that can be used by the policymakers to determine the appropriate levels of incentive programs that would foster growth in renewable energy investment in commercial buildings in support of NZEB policy goals. Numerical results of implementation of the model for commercial buildings with different characteristics show that incentive program parameters have threshold levels that promote NZEB. The thresholds depend on the annualized cost of the RE system and the cost of do nothing case (when all electricity comes from the utility).

Even though we investigated policy design based on the building types, we have shown later in the results that even within a given type of buildings, each building may have a different potential to invest in RE based on owner's financial status (credit rating and expected ROI). The presented framework can be used by the policymakers to measure the potential number of classes of commercial buildings for which RE investment is financially viable for given incentives and regulations.

An extension of this framework can be done where more data on the aforementioned classes of commercial buildings is available for a region. This data should include the annual load and available area for RE installation for buildings in each class. The load and area can be used to determine the potential RE investment in a building given enough incentives. Hence, instead of a table of positive and negative indications in response to the available incentives (see Table 17), we will have a table of potential total RE investment (in MW) in each class of commercial buildings in a region. With that, the policymaker can select incentive level to maximize the total amount of RE investment in that region, given their budget limit on RE incentives.

Investigating levelized cost of electricity (LCOE) is another possible approach to find the optimal threshold for incentive parameters for a building. Obviously, the LCOE of the on-site generated power decreases where more incentive is provided. At a point where the LCOE equals electricity price in the grid (grid parity), the building will invest in RE generation up to NZE level.

While RE investment has many long term advantages, if the policymakers' goal is to increase the number of buildings that reach NZE status, they should prioritize the classes of buildings to incentivize based on their potential to reach NZE status. Our modeling framework can be used to identify the desirable building types and classes through which RE investment can be maximized.

REFERENCES

[1] A. Ghalebani and T. K. Das, "Design of financial incentive programs to promote net zero energy buildings," *IEEE Transactions on Power Systems*, vol. PP, no. 99, pp. 1–10, 2016.

[2] R. Belfkira, L. Zhang, and G. Barakat, "Optimal sizing study of hybrid wind/pv/diesel power generation unit," *Solar Energy*, vol. 85, no. 1, pp. 100–110, 2011.

[3] A. J. Marszal, P. Heiselberg, J. Bourrelle, E. Musall, K. Voss, I. Sartori, and A. Napolitano, "Zero energy building–a review of definitions and calculation methodologies," *Energy and Buildings*, vol. 43, no. 4, pp. 971–979, 2011.

[4] S. Kahn, T. Kimbis, *et al.*, "U.S. solar market insight report, Q3 2014 executive summary," *GTM Research and SEIA*.

[5] A. W. E. A. A. D. Services, "U.S. wind industry third quarter 2014 market report," *American Wind Energy Association*, 2014.

[6] F. C. M. Z. Friedman, Ardani, "Benchmarking non-hardware balance-of-system (soft) costs for u.s. photovoltaic systems, using a bottom-up approach and installer survey second edition," *National Renewable Energy Laboratory (NREL)*, 2013.

[7] C. Gellings, "Estimating the costs and benefits of the smart grid: a preliminary estimate of the investment requirements and the resultant benefits of a fully functioning smart grid," *Electric Power Research Institute (EPRI), Technical Report (1022519)*, 2011.

[8] V. Nanduri and T. K. Das, "A survey of critical research areas in the energy segment of restructured electric power markets," *International Journal of Electrical Power & Energy Systems*, vol. 31, no. 5, pp. 181–191, 2009.

[9] E. Drury, T. Jenkin, D. Jordan, and R. Margolis, "Photovoltaic investment risk and uncertainty for residential customers," *Photovoltaics, IEEE Journal of*, vol. 4, no. 1, pp. 278–284, 2014.

[10] C. Trueblood, S. Coley, T. Key, L. Rogers, A. Ellis, C. Hansen, and E. Philpot, "PV measures up for fleet duty: Data from a tennessee plant are used to illustrate metrics that characterize plant performance," *Power and Energy Magazine, IEEE*, vol. 11, no. 2, pp. 33–44, 2013.

[11] K. N. Reddy and V. Agarwal, "Utility-interactive hybrid distributed generation scheme with compensation feature," *Energy Conversion, IEEE Transactions on*, vol. 22, no. 3, pp. 666–673, 2007.

[12] "Energy rebates, incentives, and taxes." www.dsireusa.org, Last visited in Feb 2015.

[13] J. Coughlin and K. S. Cory, *Solar photovoltaic financing: residential sector deployment*. Citeseer, 2009.

[14] R. Huang, S. H. Low, U. Topcu, K. M. Chandy, and C. R. Clarke, "Optimal design of hybrid energy system with pv/wind turbine/storage: A case study," in *Smart Grid Communications (SmartGridComm), 2011 IEEE International Conference on*, pp. 511–516, IEEE, 2011.

[15] H. Xu, U. Topcu, S. H. Low, C. R. Clarke, and K. M. Chandy, "Load-shedding probabilities with hybrid renewable power generation and energy storage," in *Communication, Control, and Computing (Allerton), 2010 48th Annual Allerton Conference on*, pp. 233–239, IEEE, 2010.

[16] P. Nema, R. Nema, and S. Rangnekar, "A current and future state of art development of hybrid energy system using wind and pv-solar: A review," *Renewable and Sustainable Energy Reviews*, vol. 13, no. 8, pp. 2096–2103, 2009.

[17] "Version 2014.11.24 system advisor model (sam)." https://sam.nrel.gov.

[18] C. Marnay, G. Venkataramanan, M. Stadler, A. S. Siddiqui, R. Firestone, and B. Chandran, "Optimal technology selection and operation of commercial-building microgrids," *Power Systems, IEEE Transactions on*, vol. 23, no. 3, pp. 975–982, 2008.

[19] H. Yang, W. Zhou, L. Lu, and Z. Fang, "Optimal sizing method for stand-alone hybrid solar–wind system with lpsp technology by using genetic algorithm," *Solar energy*, vol. 82, no. 4, pp. 354–367, 2008.

[20] G. Dalton, D. Lockington, and T. Baldock, "Feasibility analysis of renewable energy supply options for a grid-connected large hotel," *Renewable Energy*, vol. 34, no. 4, pp. 955–964, 2009.

[21] L. Kuznia, B. Zeng, G. Centeno, and Z. Miao, "Stochastic optimization for power system configuration with renewable energy in remote areas," *Annals of Operations Research*, vol. 210, no. 1, pp. 411–432, 2013.

[22] A. Danandeh, L. Zhao, and B. Zeng, "Job scheduling with uncertain local generation in smart buildings: Two-stage robust approach,"

[23] T. Logenthiran and D. Srinivasan, "Short term generation scheduling of a microgrid," in *TENCON 2009-2009 IEEE Region 10 Conference*, pp. 1–6, IEEE, 2009.

[24] G. Cardoso, M. Stadler, A. Siddiqui, C. Marnay, N. DeForest, A. Barbosa-Póvoa, and P. Ferrão, "Microgrid reliability modeling and battery scheduling using stochastic linear programming," *Electric power systems research*, vol. 103, pp. 61–69, 2013.

[25] E. Calabrò, "An algorithm to determine the optimum tilt angle of a solar panel from global horizontal solar radiation," *Journal of Renewable Energy*, vol. 2013, 2013.

[26] K. Nishioka, T. Hatayama, Y. Uraoka, T. Fuyuki, R. Hagihara, and M. Watanabe, "Field-test analysis of pv system output characteristics focusing on module temperature," *Solar Energy Materials and Solar Cells*, vol. 75, no. 3, pp. 665–671, 2003.

[27] S. Diaf, M. Belhamel, M. Haddadi, and A. Louche, "Technical and economic assessment of hybrid photovoltaic/wind system with battery storage in corsica island," *Energy Policy*, vol. 36, no. 2, pp. 743–754, 2008.

[28] P. Rocha and T. K. Das, "Finding joint bidding strategies for day-ahead electricity and related markets," in *Handbook of Networks in Power Systems I*, pp. 61–88, Springer, 2012.

[29] E. Skoplaki and J. Palyvos, "On the temperature dependence of photovoltaic module electrical performance: A review of efficiency/power correlations," *Solar energy*, vol. 83, no. 5, pp. 614–624, 2009.

[30] D. Y. Goswami, F. Kreith, and J. F. Kreider, *Principles of solar engineering*. CRC Press, 2000.

[31] R. Hendron and C. Engebrecht, *Building America house simulation protocols*. National Renewable Energy Laboratory, 2010.

[32] http://en.openei.org/datasets/files/961/pub.

[33] `http://www.wholesalesolar.com`(Last visited in Feb 2015).

[34] N. Blair, A. P. Dobos, J. Freeman, T. Neises, M. Wagner, T. Ferguson, P. Gilman, and S. Janzou, "System advisor model, sam 2014.1. 14: General description," tech. rep., NREL Report No. TP-6A20-61019, National Renewable Energy Laboratory, Golden, CO, 2014.

[35] E. Independence, "Security act of 2007," *Public Law*, vol. 110, no. 140, p. 19, 2007.

[36] B. Obama, "Federal leadership in environmental, energy, and economic performance," *Executive Order (13514) of October*, vol. 5, 2009.

[37] E. Parliament and the Council of 19 May 2010 on the energy performance of buildings, "The directive 2010/31/eu," *Official Journal of the European Union*, vol. 53, 2010.

[38] D. Crawley, S. D. Pless, and P. A. Torcellini, *Getting to net zero*. National Renewable Energy Laboratory, 2009.

[39] "Section 1703 loan program." http://energy.gov/lpo/services/section-1703-loan-program, 2015.

[40] M. Stadler, A. Siddiqui, C. Marnay, H. Aki, and J. Lai, "Control of greenhouse gas emissions by optimal DER technology investment and energy management in zero-net-energy buildings," *European Transactions on Electrical Power*, vol. 21, no. 2, pp. 1291–1309, 2011.

[41] the National Institute of Building Sciences, "A common definition for zero energy buildings," *DOE: Energy Efficiency and Renewable Energy*, 2015.

[42] M. Deru, K. Field, D. Studer, K. Benne, B. Griffith, P. Torcellini, B. Liu, M. Halverson, D. Winiarski, M. Rosenberg, *et al.*, "U.S. department of energy commercial reference building models of the national building stock," 2011.

[43] "Tampa electric - net metering." www.psc.state.fl.us/utilities/electricgas, 2014.

[44] S. E. I. Association *et al.*, "U.S. solar market insight report Q1 2015, executive summary," 2015.

[45] S. Wilcox and W. Marion, *Users manual for TMY3 data sets*. National Renewable Energy Laboratory Golden, CO, 2008.

[46] "Sam 2014.11.24 version of system advisor model." https://sam.nrel.gov.

[47] S. H. Madaeni, R. Sioshansi, and P. Denholm, "How thermal energy storage enhances the economic viability of concentrating solar power," *Proceedings of the IEEE*, vol. 100, no. 2, pp. 335–347, 2012.

[48] R. Sioshansi and P. Denholm, "The value of concentrating solar power and thermal energy storage," *Sustainable Energy, IEEE Transactions on*, vol. 1, no. 3, pp. 173–183, 2010.

[49] NREL, "The national renewable energy lab." http://www.greenstar.org/NREL.htm.

[50] Kaggle, "Kaggle competition." http://www.kaggle.com/c/ams-2014-solar-energy-prediction-contest.

[51] NetCDF, "Netcdf." http://www.unidata.ucar.edu/software/netcdf.

[52] R. Tibshirani, "Regression shrinkage and selection via the lasso," *Journal of the Royal Statistical Society. Series B (Methodological)*, pp. 267–288, 1996.

APPENDICES

Appendix A An Optimization Model for Operation of Concentrating Solar Power Plant: A Case Study[2]

A.1 Background and Problem Statement

Uncontrolled variability of distributed green energy generation from solar power is 10%/s. Where as the non-renewable energy generation like coal and natural gas has rare uncontrolled variability.[10]. TES systems are being considered as a viable option to hedge against the intermittency of the solar power resource. In the other hand, the variable (Time Of Day) price of electricity in the grid may make the TES even a profitable option to invest as the system can save thermal power and generate electricity during peak hours. If the CSP is directly used to support local demand and is the only power generator on site, then having a TES would be necessary to satisfying the reliability, i.e., meet the demand whenever sun light is not available. Although having non-renewable generators, such as diesel, may increase reliability of the system in the stand alone micro grid with a lower cost but is not an environmentally responsible solution.

The proposed approach will help making CSP viable in view of economic feasibility and operating efficiency. Based on weather data and time-based rates of grid power, the model optimally sizes the TES and how to operate it hourly. The model aims at maximizing the annual profit of the CSP. The optimal operation decisions by our model are as follows; 1) Time and level of charging and discharging the thermal energy storages, 2) Time and amount of thermal power to send to the power block. System Advisor Model (SAM) software, version

[2]This work is partially a course project for Dr. Goswami's class, Solar Energy and Applications, in Fall 2014.

2014.11.24 developed by NREL [46], is being used to simulate output thermal power of the USF microCSP. The simulation is based on typical meteorological data of Tampa-Fl (hourly solar radiation and ambient temperature) in addition to the characteristics of the solar field, solar collectors, heat collection elements (receivers), and the power block.

We have developed a MIP model in GAMS (The General Algebraic Modeling System, a high-level modeling system for mathematical programming and optimization). The MIP model is based on the model developed by R Sioshansi and colleagues [47], [48]. The MIP model uses the data output from SAM as input parameter to do the optimization on TES. The output of the MIP model is the annual generated electricity of the power block given the capacity of the TES. There are two methods to measure the capacity of TES, 1- Size of the TES in kWh, 2- Number of hours that the TES can support the power block running in its full capacity. In this project we used the second way, number of hours, for the size of the TES. The optimal hourly operation of a CSP is found by the MIP model for different sizes of the TES. Knowing the capital cost of the TES, one can determine the optimal size of the TES from the MIP results. For a given optimal size of the TES, now we can use the MIP outputs as the operation plan of the system under fluctuating solar radiation and real time price of electricity. We believe that our system, with CPLEX implementable solution strategies for its underlying models, will empower the CSP across the world, with or without smart grid infrastructure, to increase the profitability of their current powerplants. In the section A.2, the MIP problem formulation is being presented. In section A.3, we provided the computational results of the model based on the USF microCSP.

A.2 Mathematical Formulation

A.2.1 Nomenclature

Table A.1: Nomenclature used in appendix A

Symbol	Meaning
	Indices
t	Time in hours , $t \in \{0, .., 8760\}$
j	Auxiliary indices for time (t)
	Decision Variables
e_t	Electric energy sold in hour t ($kWhe$)
l_t	Storage level of TES at end of hour t ($kWht$)
s_t	Energy charged into TES in hour t ($kWht$)
d_t	Energy discharged from TES in hour t ($kWht$)
τ	Energy put into power block in hour t ($kWht$)
	Calculated Variables
r_t	Binary, $r_t = 1$ if power block is started in hour t
u_t	Binary, $u_t = 1$ if power block is on in hour t
μ_t	Auxiliary binary variable used for linearized constraints number (A.7-A.11)
ν_t	Auxiliary variable used for linearized constraints number (A.7-A.11), $\nu_t = \tau_t \mu_t$
	Input Parameters
η	Capacity of TES (hours of storage)
ϕ	Roundtrip TES efficiency (%)
ρ	Hourly energy retain in TES (%)
c	Operating cost estimate for generated electricity ($\$/kWhe$)
$\overline{d}$	TES discharge limit ($kWht$)
$\overline{s}$	TES charge limit ($kWht$)
e^{SU}	Power block startup energy usage ($kWht$)
e^{SF}	Thermal energy output from the solar field ($kWht$)
τ^-	Min. operating level of power block ($kWht$)
τ^+	Max. operating level of power block ($kWht$)
τ^K	Minimum thermal power to the power block that can generate electricity based on the heat curve($kWht$)
u^-	Minimum up time of power block (hr)
M_t	Grid electricity price ($\$/kWhe$) at t
B	A relatively very large number
γ	Parasitic proportional load of the power block(%)
a	Coefficient in the power block heat rate linear function (a constant based on the power block)
b	Intercept in the power block heat rate linear function (a constant based on the power block)

A.2.2 Problem Formulation

We have developed a Mixed Integer Programming (MIP) model and solved using CPLEX solver in GAMS. It is solved in order to find optimal level of hours of TES and optimal control strategies to yield the maximum annual revenue. Hereby we provided the objective function and constraints of the MIP model.

$$max \sum_t (M_t - c)e_t \tag{A.1}$$

$$s.t.\ l_t = \rho l_{t-1} + s_t - d_t \quad ,\forall t \tag{A.2}$$

$$l_t \leq \eta \overline{s} \quad ,\forall t \tag{A.3}$$

$$s_t \leq \overline{s} \quad ,\forall t \tag{A.4}$$

$$d_t \leq \overline{d} \quad ,\forall t \tag{A.5}$$

$$s_t - \phi d_t + \tau_t + e^{SU} r_t \leq e^{SF} \quad ,\forall t \tag{A.6}$$

$$\nu_t \leq \tau_t \quad ,\forall t \tag{A.7}$$

$$\nu_t \leq B\mu_t \quad ,\forall t \tag{A.8}$$

$$\nu_t \geq \tau_t - (1 - \mu_t)B \quad ,\forall t \tag{A.9}$$

$$e_t \leq (1 - \gamma)(a\nu_t - b\mu_t + (1 - \mu_t)B \quad ,\forall t \tag{A.10}$$

$$e_t \leq \mu_t B \quad ,\forall t \tag{A.11}$$

$$\tau_t \leq \tau^+ u_t \quad ,\forall t \tag{A.12}$$

$$\tau_t \geq \tau^- u_t \quad ,\forall t \tag{A.13}$$

$$r_t \geq u_t - u_{t-1} \quad ,\forall t \tag{A.14}$$

$$u_t \geq \sum_{j=t-u^-}^{t} r_j \quad , \forall t \tag{A.15}$$

$$l_t, s_t, d_t, \tau_t, \nu_t \ \in \mathbb{R}^+, e_t \in \mathbb{R}, r_t, u_t, \mu_t \in \{0, 1\} \tag{A.16}$$

The objective function (A.1) is the revenue from sale of electricity minus the estimated operating cost. The constraint in (A.2) hourly updates the TES storage level. Constraints (A.3,A.4,A.5) set limit on storage level and also on charging and discharging of the TES. In (A.6) we ensure that the total thermal energy flow in the system at any time is always less than the thermal power output of the solar field in addition to the discharged energy from the TES. We assumed a piecewise linear function for the power block heat rate function. In order to have it in the set of MIP constraints, we made it linear by defining constraints (A.7-A.11). In general, if the heat rate function is piecewise linear, we have,

$$e_t = \begin{cases} 0 & \tau_t \leq \tau^K \\ a\tau_t + b & \tau_t \geq \tau^K \end{cases}$$

Constraints (A.12,A.13) determine the acceptable range for thermal power input to the power block. Since there is a startup energy consumption in the power block, constraint (A.14) defines the power block startup hours. We can also enforce a minimum up-time requirement on the power block by the constraint (A.15).

A.3 Computational Study

A.3.1 CSP Characteristics

Using the model, we optimized the size and hourly operation of a TES for the microCSP (parabolic solar trough CSP) at USF. Different characteristics of the site has been measured by visiting the plant and also gathered from the CERC members. The CSP properties has been used as inputs to the SAM software to simulate the solar field. Simulation's result are hourly thermal energy output of the solar field and the hourly output electricity from the power block. Some important measures of the site, i.e. ,solar field and power block characteristics, are given in Table A.2 and A.3, respectively.

Table A.2: Solar field characteristics

Number of Troughs per Row	14
Number of Rows	14
Row Spacing Center to Center	$2.4m$
Distance Between Troughs in a Row	$0.25m$
Solar Collector Assembly (SCA) Length	$52m$
SCA Aperture	$1.65m$
SCA Aperture Reflective Area	$80m^2$
Solar Field Reflective Area	$1120m^2$
Average Focal Length	$0.65m$
Heat transfer fluid (HTF)	Water-Glycol
Solar Field Inlet Temp.	$26°C$
Solar Field Outlet Temp.	$97°C$

Table A.3: Power block characteristics

Type of Power Cycle	Organic Rankine Cycle (ORC)
Gross Electricity Output	65 kW-e
Estimated Gross to Net Conversion	0.9
Min. Thermal Input	400 kW-t
Max. Thermal Input	825 kW-t
Startup thermal power	50 kWht
Rated Cycle Conversion Efficiency	8.3%

A.3.2 Local Weather Data

The hourly historical data on incoming solar radiation and ambient temperature is available on SAM Weather Data (by NREL).Given the location of the site, we used the typical meteorological year (TMY) data for Tampa, FL.

A.4 SAM Simulation Outputs

Provided the input parameters of this case study, SAM simulated the CSP. Among different outputs of the simulation, we care the most for the following results. These data has been used to find the power block heat rate function (see the next subsection). This function as well as the thermal energy available form the solar field (e_t^{SF}) are used as inputs to the MIP model.

- Hourly thermal energy output from the solar field (kWht)
- Hourly gross electricity generation in power block kWhe)

A.5 Heat Rate Curve Function of the Power Block

Given the SAM simulation results, the following hourly data has been used in order to estimate the heat rate curve function of the power block, 1-Thermal energy available from the solar field ($e_t^{SF}, kWht$), 2- Gross electric production from the solar resource ($e_t, kWhe$). So we are looking for $f(.)$ such that, $e_t = f(e_t^{SF})$.

R data analytics language is used to analyze heat-power data and to find the function for the heat curve. First, the zero power output has been eliminated. Because we know that the thermal input to the power block is in the range of 400-820 kWt . Also there is a 50 kWh of thermal energy as power block startup energy. So we just need to find the function

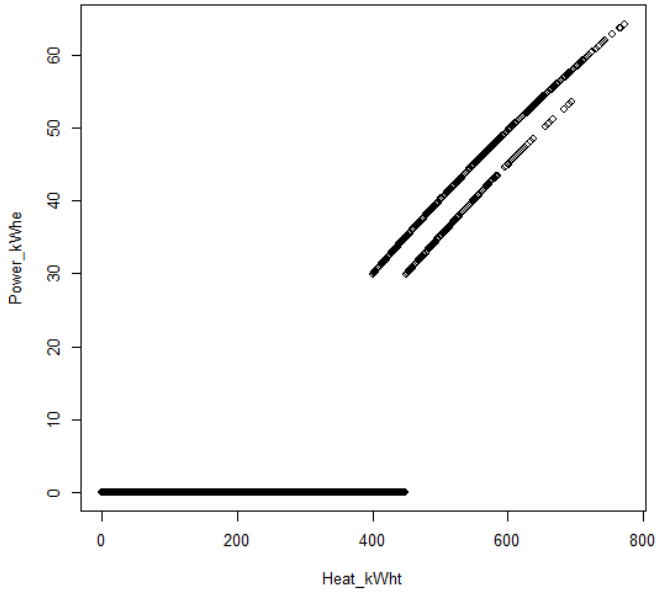

Figure A.1: Electricity output of the power block vs input thermal energy

for those hours without startup power loss. The next step is ANOVA. It showed that we can fit a linear model on the data (Fig.A.2).

Then the linear regression is fitted (Fig.A.3) and the heat rate linear function of the power block is $e_t = 0.0938e_t^{SF} - 6.9743$.

From this function, we can also estimate capacity of the TES to make the power block working operate at its maximum load using energy from storage alone for one hour. Let's assume that the TES system has the same power capacity for charging ($\overline{s}$) and discharging ($\overline{d}$). That is equivalent to one hour capacity of TES.

$$65 = 0.0938\overline{s} - 6.9743 \qquad \therefore \overline{s}, \overline{d} = 767.32\ kWht$$

```
> anova(Curve)
Analysis of Variance Table

Response: Power
           Df Sum Sq Mean Sq F value    Pr(>F)
Heat        1  46182   46182  494129 < 2.2e-16 ***
Residuals 657     61       0
---
Signif. codes:  0 '***' 0.001 '**' 0.01 '*' 0.05 '.' 0.1 ' ' 1
> summary(Curve)

Call:
lm(formula = Power ~ Heat)

Residuals:
     Min       1Q   Median       3Q      Max
-1.34930 -0.19585  0.08829  0.25439  0.31687

Coefficients:
             Estimate Std. Error t value Pr(>|t|)
(Intercept) -6.9742746  0.0739972  -94.25   <2e-16 ***
Heat         0.0937986  0.0001334  702.94   <2e-16 ***
---
Signif. codes:  0 '***' 0.001 '**' 0.01 '*' 0.05 '.' 0.1 ' ' 1

Residual standard error: 0.3057 on 657 degrees of freedom
Multiple R-squared:  0.9987,    Adjusted R-squared:  0.9987
F-statistic: 4.941e+05 on 1 and 657 DF,  p-value: < 2.2e-16
```

Figure A.2: R software outputs: ANOVA and linear regression summary on thermal energy and output electricity data

A.6 Optimal Sizing of the TES

At this point, we want to find the impact of different capacity of the the thermal energy storage (TES) ,in terms of number of hours of storage, on the revenue. The required parameters, as described in section A.2, are fed into the MIP model in GAMS to be solve the problem by CPLEX solver. The MIP model is being solved for different number of hours of TES from zero,i.e., CSP without TES, to nine hours of TES capacity.

The results of sizing the TES are shown in Fig.A.4-A.7. In Fig.A.4 we can see the useful thermal energy input to the power block is doubled by having at least one hour of TES comparing to the CSP without TES. The reason is, the power block rejects any amount of thermal energy below the $\tau^{-}(400kWht)$ level. We can also observe from Fig.A.4 that having 2 hours of TES or more does not make a meaningful improvement in the amount of input power to the power block for this CSP. So consequently electricity output from power

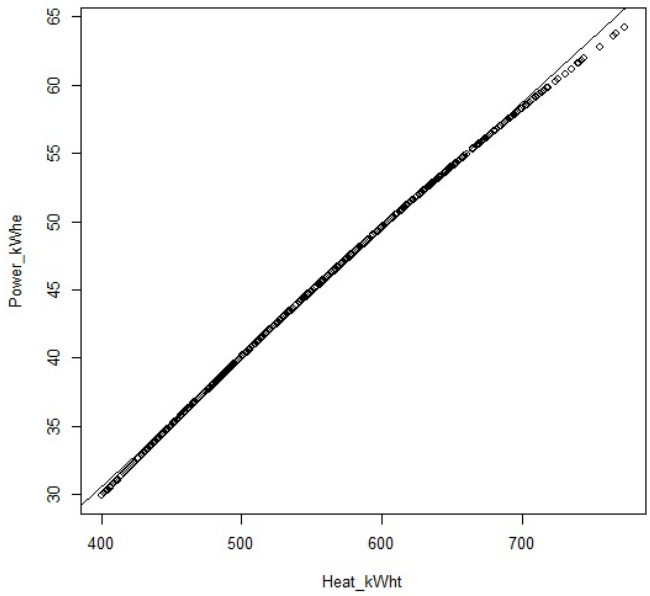

Figure A.3: Heat rate curve of the power block

block will not increase if 2 hours or more of TES is used comparing to just 1 hour capacity (Fig. A.5).

Although the total electricity output of the plant is not changing for different TES sizes (of 1 hour or more), annual revenue is increasing with increasing the capacity of TES (Fig. A.6 and Fig. A.7). The additional revenue given the same annual thermal energy input is because of the more flexibility in operation that a larger TES gives to the controller. More details on operation are provided in the next subsection.

The ultimate decision on the size of the TES is based on the capital costs of the TES system and its physical characteristics. If the price and properties of TES optins is being provided, the MIP model can be updated to find the optimal TES size. For this project, we compromised the physical and economic constraints, we picked 4 hours as the size of the

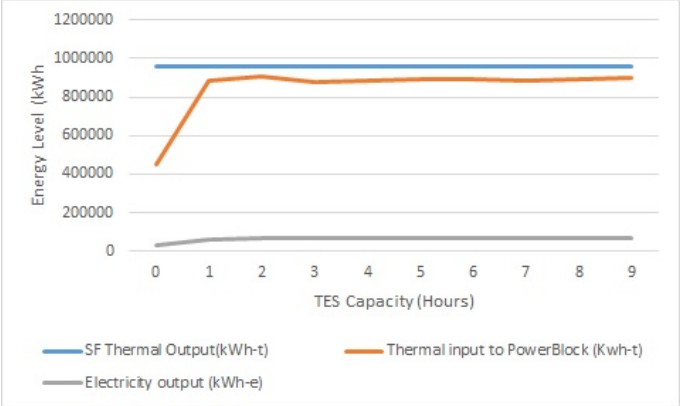

Figure A.4: Energy to power block

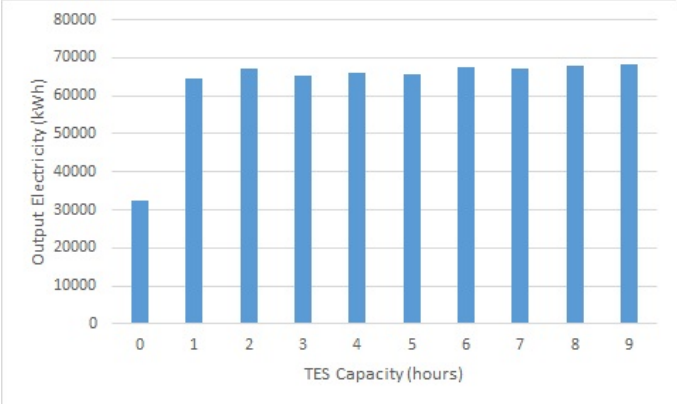

Figure A.5: Electricity output (kWhe)

TES. That is only because there is still a meaningful additional annual revenue by adding the 4th hour of capacity to the TES system (Fig. A.7).

A.7 Optimal Operation Plan

The electricity output from this microCSP can be used at USF or sold back to the main grid under NetMetering policy. In other words, USF needs to satisfy its demand by purchasing power from the local utility company, TECO, or a combination with the output power from its CSP. Let's assume the electricity price is under the time of day price tariff (Look at Fig.A.8). In this case generating electricity during hours with on-peak price may

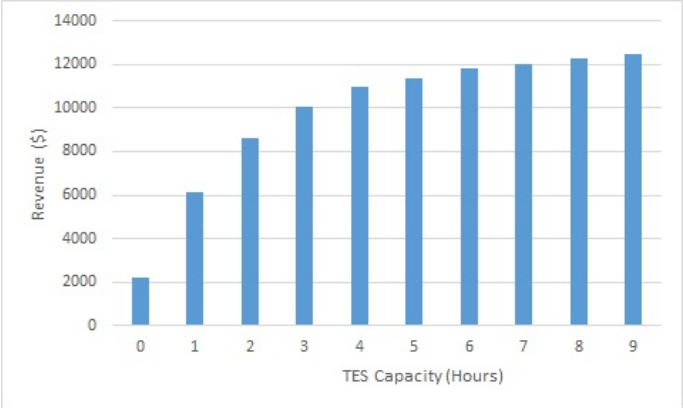

Figure A.6: Revenue

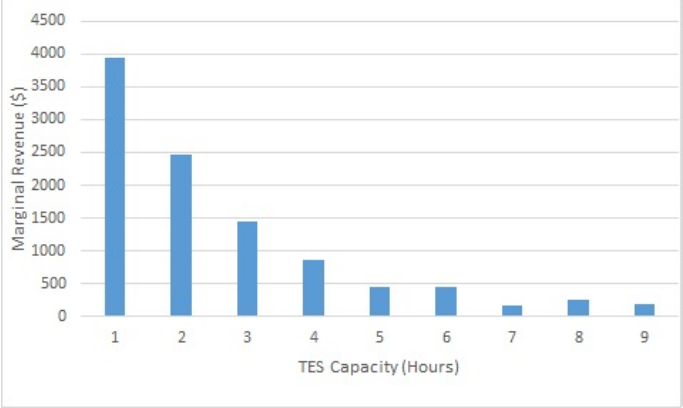

Figure A.7: Marginal revenue for added TES hour

lead to higher revenue or higher cost savings. The MIP model considers all the constraints on energy flows in the system and the results are feasible hourly control actions. As an example, a snapshot of a week of operation of the microCSP with TES (capacity of 4 hours) is shown in Fig.A.9. For the first week of January, Fig. A.9 shows a typical energy circulation in the system. The thermal power is being charged to the TES during the weekend, because it is off-peak hours and the price is low.

As there is a start up thermal energy usage by the power block, the optimal operations tends to minimize the number of startups as well. System discharges the TES and generates

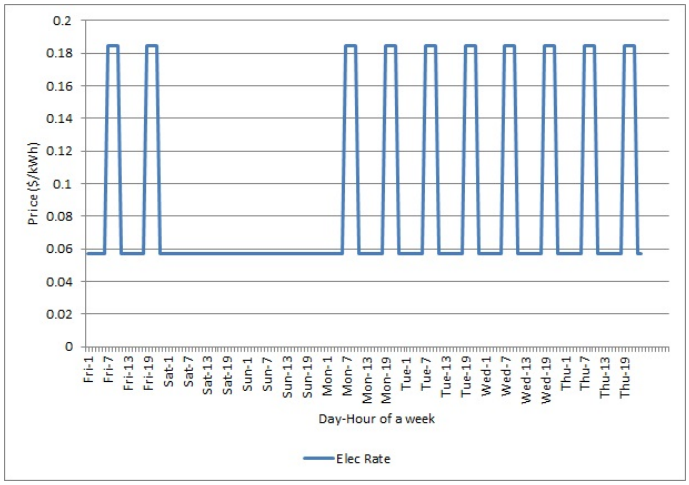

Figure A.8: Time of day price of electricity

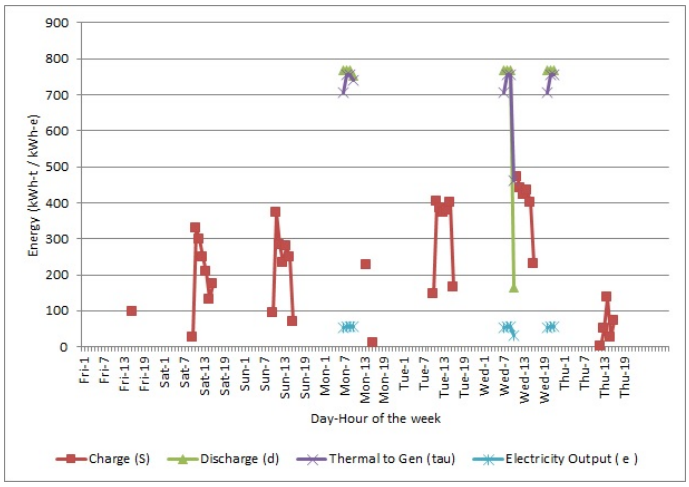

Figure A.9: A typical optimal operation plan (1st week of January)

electricity in power block during peak hours and charges thermal energy the rest of the hours, given the TES capacity (Fig.A.10).

A.8 Conclusion and Future Work

The proposed model can be used by a CSP controller to optimally operate the hybrid system of CSP and TES. The results show, MIP optimization of the operation of the system significantly increases the revenue from the power sale. This model is also easily expandable

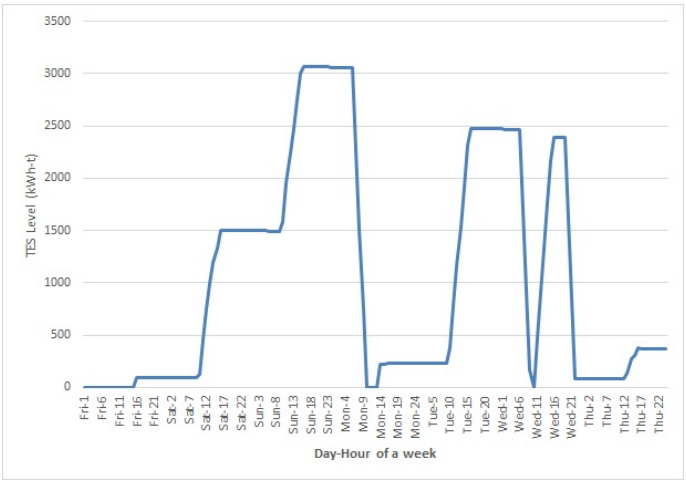

Figure A.10: Level of thermal energy stored in the TES

to use for a stand-alone micro grid to support a local electricity/theraml power demand. The next step to extend the model is including stochastic parameters of prices and solar resources. We want to consider uncertainty in the electricity price and short term solar radiation. Also the life time of the system can be considered as a variable dependent to its activity. As the parabolic trough can be turned down during low radiation periods, the model may consider this as an operation decision opportunity. The optimal operation strategy aims at maximizing the lifetime of the CSP as a second objective as well.

Appendix B A Predictive Model for Daily Solar Energy Using Gradient Boosting Method: AMS 2013-2014 Solar Energy Prediction Contest[3]

B.1 Introduction

Renewable energy sources have gained a significant popularity recently. A typical example is solar power which is the conversion of sunlight into electricity, either directly using photovoltaics (PV), or indirectly using concentrated solar power (CSP). Solar energy has a high potential to cover our electricity needs, according to [49] The amount of sunlight that falls on the United States in one day has more than twice the annual energy consumption.

Moreover, renewable energy sources have many environmental advantages over fossil fuels in electricity generation. While combustion of fossil fuels results in large volume of green gas emissions, renewable energy source are very much clean.

However, the green energy generation is very uncertain by nature and depends a lot on the weather conditions. This might affect their reliability. Electric utility companies that put renewable energy in their source portfolio need to have accurate forecasts of energy production in order to plan ahead and manage the renewable and fossil fuels and possibly other sources available. The inaccurate forecast affects the unit commitment and dispatch problems in the utility companies and could lead to large expenses for the utility.

Numerical weather prediction models are commonly used for power forecasts. And, recently, statistical and machine learning techniques are increasingly being used in conjunction with these models for more accurate forecasts [50]. In order to develop models and techniques to accurately predict the renewable power generation, the American Meteorological

[3]This work is a project done in collaboration with Anna Danandeh and Mehrnaz Abdollahian.

Society organized a competition. Three Committees of Artificial Intelligence Applications to Environmental Science, Probability and Statistics, and Earth and Energy of this society were involved in the "2013-2014 Solar Energy Prediction Contest" and $10000 worth of prizes are sponsored by EarthRisk Technologies, Inc. The competition was on Kaggle website and open for public. We chose this problem due to the high applicability of it as our course project.

This report contains our ideas and the methodologies that we applied for this project and is organized as follows: Section B.2 describes the problem and provides a simple presentation; section B.3 explains the solution approaches that we took; the model results, along with some discussion on the successful and unsuccessful approaches are shown in Section B.4; and finally section B.5 summarizes the project and talks about what we learnt during the project to conclude the report.

B.2 Problem Statement

B.2.1 Problem Overview

The objective in this project is to discover the best statistical and machine learning techniques that can predict short term solar energy production. The scope of the project is Oklahoma state. In particular, we are interested in predicting the solar power generation of 98 solar farms with an uneven distribution though out the state. Here we call these solar farms Mesonets. The Mesonet sites all have the same instrumentation for measuring solar radiation and are regularly inspected and calibrated, therefore the only differences between them should be due to environmental factors and weather forecast. For each Mesonet we know the daily electricity generation and its geographical location.

The numerical weather prediction data comes from the NOAA/ESRL Global Ensemble Forecast System (GEFS) Reforecast Version 2. This Data include 11 ensemble models and provides 15 weather factors including precipitation, long/ short wave radiation, air pressure, humidity, and total cloud cover. For the complete list of please refer to Table B.4. The forecast timesteps are 12, 15, 18, 21, and 24 global time which is equivalent to 6AM-6PM central time. More information about the data will be provided in the next subsection. Figure B.11 depicts the relative distance between locations of the Mesonet sites and the GEFS points and provides a visualization of the grid.

Table B.4: Weather condition variables included in the ensemble models

Variable	**Description**	**Unit**
apcp_sfc	3-Hour accumulated precipitation at the surface	kg m-2
dlwrf_sfc	Downward long-wave radiative flux average at the surface	W m-2
dswrf_sfc	Downward short-wave radiative flux average at the surface	W m-2
pres_msl	Air pressure at mean sea level	Pa
pwat_eatm	Precipitable Water over the entire depth of the atmosphere	kg m-2
spfh_2m	Specific Humidity at 2 m above ground	kg kg-1
tcdc_eatm	Total cloud cover over the entire depth of the atmosphere	%
tcolc_eatm	Total column-integrated condensate over the entire atmos.	kg m-2
tmax_2m	Maximum Temperature over the past 3 hours at 2 m above the ground	K
tmin_2m	Mininmum Temperature over the past 3 hours at 2 m above the ground	K
tmp_2m	Current temperature at 2 m above the ground	K
tmp_sfc	Temperature of the surface	K
ulwrf_sfc	Upward long-wave radiation at the surface	W m-2
ulwrf_tatm	Upward long-wave radiation at the top of the atmosphere	W m-2
uswrf_sfc	Upward short-wave radiation at the surface	W m-2

For the competition, contestants were supposed to submit predictions of the total solar daily incoming solar radiation at 98 Oklahoma Mesonet sites for each day. The Mean

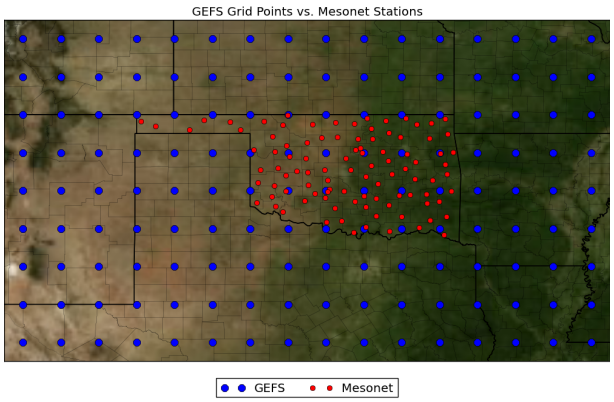

Figure B.11: Mesonets & GEFS station maps

Absolute Error (MAE) was the evaluation metric. This metric is commonly used in regression problems and by the renewable energy industry to compare forecast performance. Unlike Root Mean Squared Error, MAE does not excessively punish extreme forecasts.

$$\text{MAE} = \frac{1}{SE} \sum_{s}^{S} \sum_{e}^{E} \mid F_{se} - O_{se} \mid \tag{B.17}$$

It's important to note that there were no station-by-station comparison, so although the developed model for each station might be different from the other station, we can not see how good or bad we have done for any specific Mesonet.

B.2.2 Handling Data

Most of the contest data were provided in NetCDF4 file format. NetCDF stands for Network Common Data Form and is a set of interfaces for array-oriented data access and afreely distributed collection of data access libraries for R, C++, Java, and other languages. In order to work with the data, we used *ncdf* package in *R* and wrote some functions to read, manipulate and write data in that format [51].

Training data come from 1994-2007 and were separated into 3 files. There were two files containing all of the GEFS training data. The data are in netCDF4 files with each file holding the grids for each ensemble member at every time step for a particular variable. Each netCDF file contains the latitude-longitude grid, the timestep values and metadata listing the full names of each variable and the associated units.

Each netCDF4 file contains the total data for one of the model variables and are stored in a multidimensional array. The data includes the date, the ensemble member that the forecast comes from (As mentioned before the GEFS has 11 ensemble members with perturbed initial conditions), the forecast hour, which runs from 12 to 24 hours in 3 hour increments, and finally the latitude and longitude uniform spatial grid. There is another file that contains the total daily incoming solar energy in (J m-2) at 98 Oklahoma Mesonet sites that have been in continuous operation since January 1, 1994. The solar energy was directly measured by a pyranometer at each Mesonet site every 5 minutes and summed from sunrise to 23:55 UTC of the date listed in each column.

The third file contains the latitude, longitudes, and elevation (meters) of each Mesonet station. There were discussions about usability of elevation, and, therefore, elevation was later added to the information. Figure B.12(a) depicts hoe elevation can change the distance interpretation. Since there are up to 300 meters difference in the elevations, using one instead of the other could have an impact on the model. Public testing data will be from 2008-2012 and private testing data for a more recent period will be used for the final evaluation.

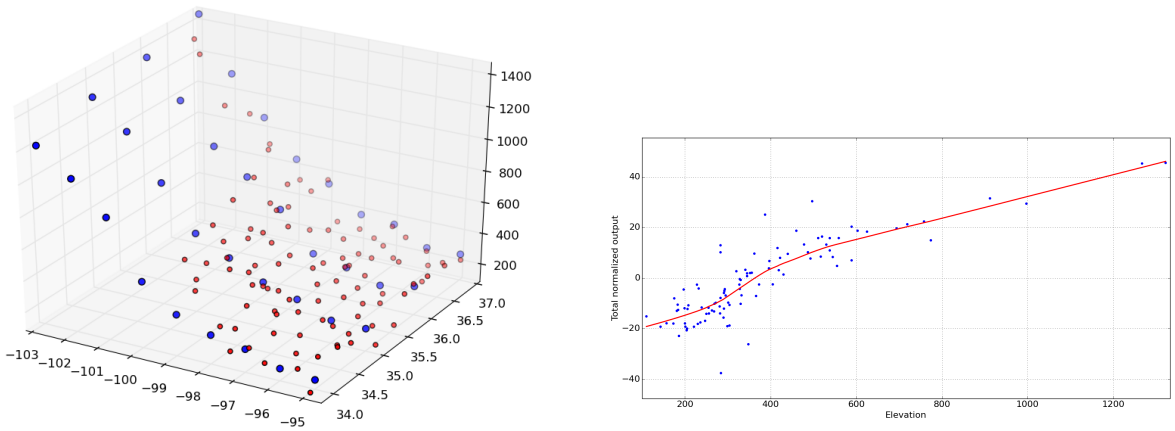

(a) Mesonets & GEFS three-dimension maps

(b) Elevation and solar energy output

Figure B.12: Elevation significance

An interesting aspect of most of data sets were the seasonality in the variables. The Figure B.13 presents the values of each weather forecasting variable for a random GEFS point from 1994 to 1996. Obviously, the seasonality comes more from the nature of the variable, since the locations are not much different, therefore, the variables in the other GEFS show similar behaviour.

The problem is a *BigData* analysis with having more 650M data cells in the training and 220M data cells in the test set. One of the ways we tried to for reducing the dimensionality of the data was taking average on ensemble models, i.e. instead of having 11 forecasts for each variable, we worked with only one value which was the average of the 11 forecasts. At that point we wanted to start with a simple model and then build on that. Later, we realized that this approach might not be a good one especially considering the evaluation metric. Taking weighted averaged based on argmin(MAE) can be a better approach which emphasized on the models that can reduce the MAE. We'll consider this idea in future.

B.3 Solution Approach

We tried two approaches, in the first approach we performed more data engineering and worked with a fewer variables in our prediction model, and then we applied LASSO method to select the most important variables in prediction. This approach was not very successful, so we did some studies and came to conclusion that it's better not to manipulate data, and instead used much higher number of variables in the prediction model which was based on GBM model which performed much better. both approaches are explained in the following subsections. In each subsection we first explain the data pre-processing steps and then for completeness, we provide a brief and general overview of the method, and then elaborate on how we utilized that method.

B.3.1 LASSO Approach

For simplicity, here we summarize the data pre-processing approach in Algorithm 1.

For each Mesonet station:
Step 1: Choose the closest 10 GEFS points with respect to the elevation and then choose the 4 closest ones based on lon/lat distance
Step 2: for each predictive variables of the Mesonet take weighted average of the selected 4 GEFS
Step 3: for each predictive variables take average of the 5 time instances in a day (6, 9, 12, 15, 18) to prepare for daily prediction
Step 4: use the resulted 15 GEFS features as covariate matrix for the given Mesonet

Algorithm 1: First data pre-processing

After preparing the variables, we applied LASSO method to choose the most significant features in the model. LASSO stands for the Least Absolute Shrinkage and Selection Operator. This method minimizes the usual sum of squared errors, with a bound on the sum of the absolute values of the coefficients [52]. LASSO is an automated feature selection like AIC

(Akaike information criterion), BIC (Bayesian information criterion) and MDL (minimum description length). The reason we picked LASSO was mainly its faster computational time for model selection. LASSO formulation is provided in B.18-B.21.

$$Find\,\hat{\beta}_{LASSO} = argmin_{\beta}\{RRS(\beta) + L_1(\beta)|D\} \tag{B.18}$$

$$s.t.\, L_1(\beta) = \lambda \sum_j |\beta_j| \tag{B.19}$$

$$RSS(\beta) \equiv \sum_i (y_i - \beta X_i)^2 \tag{B.20}$$

$$\lambda \geq 0\ \&\ D = \{(X_i, y_i)\}_{i=1}^{n} \text{is the training set} \tag{B.21}$$

We used *LARS* package in R to use LASSO. This software computes the entire LAR, LASSO or Stagewise path in the same order of computations as a single least-squares fit. In order to provide an example, variable selection for Mesonet station 1 is provided in Figure B.14. Figure B.14(a) represents the piece-wise linear profiles of lasso coefficients, as the tuning parameter $\beta/\max\beta$ is varied. A vertical line is drawn at 0.96 which is chosen by cross-validation. Figure B.14(b) demonstrates the 10-fold cross-validation that minimizes the Mean Squared Error (MSE). Based on this cross-validation, 0.96 (shown by the red vertical line) had the lowest MSE and therefore the coefficients chosen at this shrinkage level by LASSO were picked as the best ones. It can be seen that, using LASSO which minimizes the MSE, was not the best approach, especially because it was not aligned with the evaluation metric of this competition which was MAE. Therefore we switched to another model. Next, we explain our improved approach.

B.3.2 GBM Approach

Based on our experience in the first approach, we learned the importance of minimizing feature engineering. Therefore, we attempted at adding more variables to our model instead of reducing the dimensionality of the problem. Here, we briefly describe the updates we had in our data preparation:

- Instead of taking the average of hourly-weather prediction, we used them directly as part of covariate matrix, e.g. instead of taking the average of short-wave radiation in times 12, 15,18,21,24, we create short-wave-12, short-wave-15, ..., short-wave-24 and included them as variables in the model. With this change, (Number of weather features=15)$\times$(Number of forecast hours=5)=75 new variables were created.
- Instead of taking average of the 4 closest stations, we created two sets of covariates. The first set includes all those values (75$\times$4=300) and the second one was calculated by taking the distance-weighted average of 4-closet stations (75). Therefore, we added another 375 variables to the model.
- We also used other variables such as month of the year, latitude difference (between mesonet and 4-gefs stations), longitude difference (between mesonet and 4-gefs stations) and elevation difference (between mesonet and 4-gefs stations).

We should also mention that we applied two versions of GBM. Algorithm 2 describes the data engineering for the first one, and in the second model, we removed the variables created as the distance-weighted average of 4-closet stations. All the parameter setting were identical for the both version.

After being done with data processing, we chose Gradient Boosting Method (GBM) as the method. Here we briefly talk about boosting and gradient boosting method. Boosting is an ensemble technique in which learners are learned sequentially. Gradient boosting is an extension of boosting for regression convert a sequence of base (weak) learner to a complex overall predictors. In general, The GBM iteratively learns a simple regression from the data, computes residual error and then creates a new model to predict this error residual. The accuracy of the model gets better at each step for the training data. The mathematical representation of this explanation is gathered in the following algorithm:

While the error is big **Step 1:** make a set of predictions $\hat{y[i]} = mean(y)$
Step 2: find the residual error $MAEj(.) = \sum |y[i] - \hat{y[i]}|$
Step 3: adjust $\hat{y}$ to reduce the error $\hat{y[i]} = \hat{y[i]} + \alpha f[i]$ where $f[i] \approx$ gradient of the loss function
Step 4: use the resulted 15 GEFS features as covariate matrix for the given Mesonet
Algorithm 2: GBM algorithm

We used GBM with the following parameters: Number of terminal nodes in trees whichcontrols the maximum allowed level of interactionbetween variables in the model was set to 10. Increasingnumber of treeswill reduce the error on training set however setting it too high may lead to overfitting. So it's very important to pick the right number. In this model, we set the number of trees to 3000. Table B.5 and Figure B.15 demonstrate the improvement from 2000 trees to 3000, but also shows that increasing this number will not benefit that much, but will increase the computation time. Empirically using small learning rates yields dramatic improvements in model's generalization but results in an increase in the computational time. We set the Shrinkage level at 0.005.

Since our were dealing with time-series data, we could not randomly select the data sets for cross-validation. Our approach was to use a 3-fold contiguous validation with the following portions: 1) 1994-1998, 2) 1999-2003, and 3) 2004-2007.

Table B.5: Choosing the appropriate number of trees for GMB method

	distance-averaged removed		
# of trees	**4000**	**3000**	**2000**
MAE-test set 1	2,069	2,068	2,078
MAE-test set 2	1,970	1,971	1,973
MAE-test set 3	2,154	2,154	2,156
Average MAE	2,064	2,064	2,069

* All the MAE numbers should be scaled by 1000

B.4 Results

In this section we'll present the results from both models and provide a comparison and some insights.

B.4.1 Parallel Computing

Traditionally, software has been written for serial computation on a single computer having a single CPU. Running large-scale problems in this way can be really time-consuming and does not make efficient use of the resources available. Nevertheless, simultaneous using multiple compute resources or processors to solve a computational problem can overcome this disadvantage. As we mentioned in section B.2, the problem that we are solving is a Big Data Analysis problem. Especially, in the second approach where we had much more variables, solving the problem regularly would take really long time and in some cases would freeze the computer. In order to overcome this challenge, we used parallel computing. We ran the instances on a computer with Intel core i7 with 8 processors. Table B.6 shows the

average computation time for each instance. Running all the instances took 220 min when parallel computing was used vs 1274 min without it.

Table B.6: Computation time from parallel computing

Task	**Time per station**
Making the covariate matrix for the train set	20 min
Making the covariate matrix for the test set	13 min
Fitting gbm on train set	13 min

B.4.2 LASSO Approach

Since plotting the predictions for all 98 mesonets would not help much and moreover the plots are not much different, Figure B.16 presents a prediction plot for mesonet number one. The important variables given this approach were presented in Table B.7.

Table B.7: The significant variables based LASSO feature selection model

Variable	Coefficient
surface-temp	-2060958.316
max-temp	-1620213.734
Precipitable Water	-146226.1274
min-temp	-82820.01747
long-wave	-73202.42836
short-wave-surface	-2691.428577
Air pressure	-520.2017723
Total cloud	0
top-longradiation	29761.59149
short-wave	46586.61346
precipitation	111919.4944
surface-longradiation	335431.0835
Current-temp	2419263.312
condensate	2891440.81
Humidity	137972464

B.4.3 GBM Approach

Data cleaning and GBM development were described in section B.3.2. In this section we present the output of the model for mesonet number 1 in Figure B.17. The rest of mesonets show a similar behaviour. For this particular mesonet, 301 variables from 333 had non-zero influence in GBM approach. Tabel B.8 summarizes the main ones and their influence on the prediction. As you see, the variables chosen by this model make more sense comparing to the variables chosen by LASSO. The main variables are short waves radiation in different hours, which is another interesting fact that proves out second approach in considering the weather variables in all the time steps instead of simply taking an average was a correct decision. As mentioned before, considered two versions of GBM: one with 414 variables and one with fewer variables. Table B.9 represents the MAE for the three set we used for cross-validation. In each case, we tried different seeds (from one to three). We can see that the model with fewer variables outperformed the original model and also takes short computation time.

Table B.8: Variable significance based on GBM

Variable name	**Relative influence**
short.wave_21_st4	1
short.wave_24_st4	0.3712
short.wave_18_st4	0.2313
short.wave.surface_21_st4	0.0953
short.wave.surface_18_st4	0.0657
short.wave.surface_18_st3	0.0495
short.wave_18_st3	0.0412
short.wave.surface_15_st4	0.0397

Table B.9: Dimension reduction in GBM

	all 414 variables			distance-averaged removed		
Seeds	1	2	3	1	2	3
MAE-test set 1	2,060*	2,061	2,061	2,065	2,068	2,063
MAE-test set 2	1,963	1,976	1,975	1,967	1,971	1,969
MAE-test set 3	2,170	2,172	2,172	2,158	2,154	2,160
Average MAE	2,064	2,070	2,069	2,063	2,064	2,064

* All the MAE numbers should be scaled by 1000

B.4.4 Approach Comparison

In order to evaluate the efficiency of the different models we developed, we compared the evaluation metric, MAE, in each case and provided the improvement percentage at each step. The results are presented in Table B.10. As you see, using GBM compared to LASSO improved our performance drastically. This can be explained with many facts. First of all, LASSO would minimize MSE while our evaluation metric was MAE. Moreover, the data engineering that we performed in the first approach manipulated the result. Therefore, when we considered much more variables and let the model decide which variables are playing much more important role we got a better result. We can see that variable reduction was effective, but didn't drastically improved the prediction.

Table B.10: Approach comparison

Method	**Score**	**Marginal improvement**
Lasso	3E+06	-
Gbm-414 variable	2E+06	20%
Gbm-333 variable	2E+06	0.30%

B.5 Conclusion

In this report, we presented the numerical model we developed for short term prediction of solar energy generation. There were 98 solar farms (mesonets)in state of Oklahoma and

we were interested in predicting their solar energy generation. The prediction will be based on the weather condition on 144 weather stations (GEFS). For each mesonet we know the generation hisoty and geographical location and for each GEFS point, we know the location as well as 15 weather variables predicted by 11 ensemble models.

The problem is a Big Data analysis with time-series data, therefore we used parallel computing to handle such a large-scaled problem. We have tried different data engineering approaches and tested LASSO and GBM on our data. The results indicate that on this data set, we should have minimized the data manipulation, and included all the data points as variables so the model can choose the ones that have higher influence on the generation. GBM proved to be a good approach, however, there is still room for improvements.

For the future work we plan to work on our weighted averages and assign weights in a way that minimizes MAE. Also, we want to explore other prediction methods.

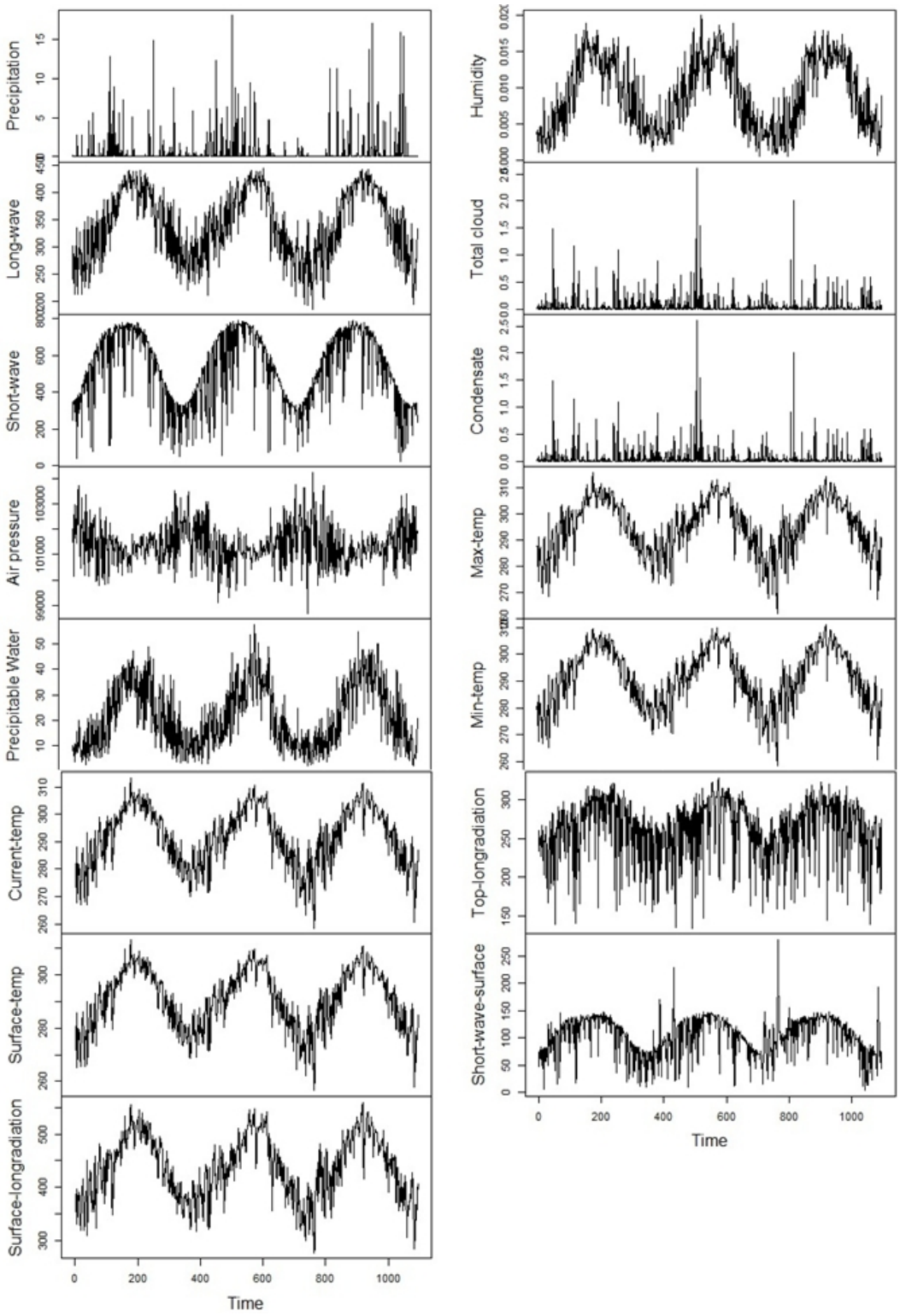

Figure B.13: 1994-1996 values of the 15 weather forecasting variables of a random GEFS point

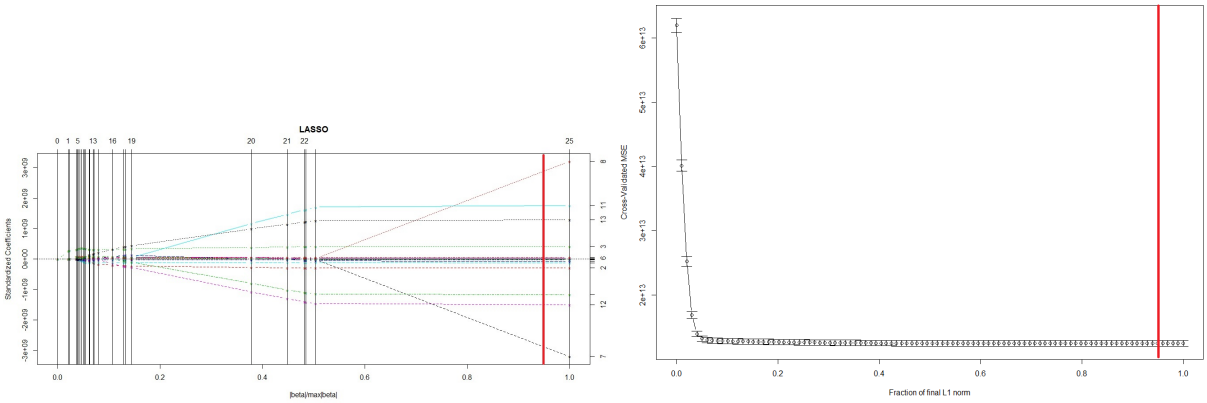

(a) LASSO coefficients plot (b) Cross-validation

Figure B.14: LASSO figures

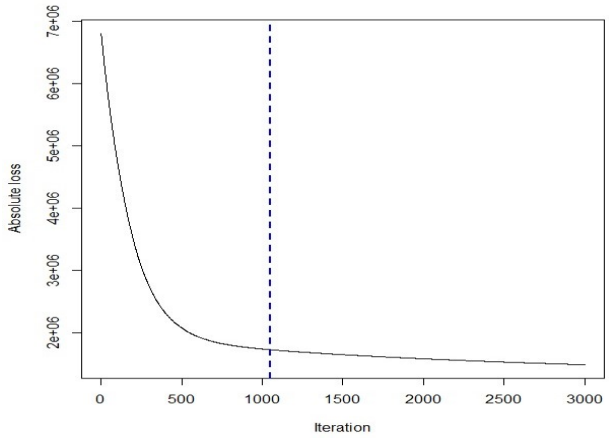

Figure B.15: Number of iterations

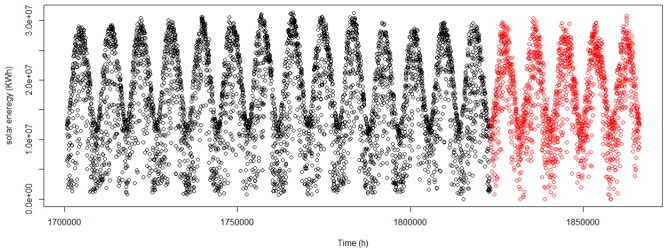

Figure B.16: A typical prediction plot- LASSO prediction for Mesonet #1

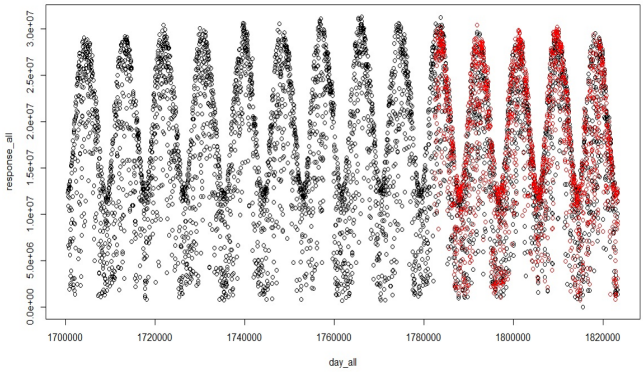

Figure B.17: A typical prediction plot- GBM prediction for Mesonet #1

Appendix C Copyright Permissions

C.1 Permission from IEEE to Reuse [1] in Chapter 3

Title: Design of Financial Incentive Programs to Promote Net Zero Energy Buildings
Author: A. Ghalebani; T. K. Das
Publication: Power Systems, IEEE Transactions on
Publisher: IEEE
Copyright © 1969, IEEE

LOGIN

If you're a copyright.com user, you can login to RightsLink using your copyright.com credentials. Already **a RightsLink user** or want to learn more?

Thesis / Dissertation Reuse

The IEEE does not require individuals working on a thesis to obtain a formal reuse license, however, you may print out this statement to be used as a permission grant:

Requirements to be followed when using any portion (e.g., figure, graph, table, or textual material) of an IEEE copyrighted paper in a thesis:

1) In the case of textual material (e.g., using short quotes or referring to the work within these papers) users must give full credit to the original source (author, paper, publication) followed by the IEEE copyright line © 2011 IEEE.
2) In the case of illustrations or tabular material, we require that the copyright line © [Year of original publication] IEEE appear prominently with each reprinted figure and/or table.
3) If a substantial portion of the original paper is to be used, and if you are not the senior author, also obtain the senior author's approval.

Requirements to be followed when using an entire IEEE copyrighted paper in a thesis:

1) The following IEEE copyright/ credit notice should be placed prominently in the references: © [year of original publication] IEEE. Reprinted, with permission, from [author names, paper title, IEEE publication title, and month/year of publication]
2) Only the accepted version of an IEEE copyrighted paper can be used when posting the paper or your thesis on-line.
3) In placing the thesis on the author's university website, please display the following message in a prominent place on the website: In reference to IEEE copyrighted material which is used with permission in this thesis, the IEEE does not endorse any of [university/educational entity's name goes here]'s products or services. Internal or personal use of this material is permitted. If interested in reprinting/republishing IEEE copyrighted material for advertising or promotional purposes or for creating new collective works for resale or redistribution, please go to http://www.ieee.org/publications_standards/publications/rights/rights_link.html to learn how to obtain a License from RightsLink.

If applicable, University Microfilms and/or ProQuest Library, or the Archives of Canada may supply single copies of the dissertation.

BACK CLOSE WINDOW